The total position-spread tensor: Spin partition

Muammar El Khatib,[1,a)] Oriana Brea,[1,2,b)] Edoardo Fertitta,[3,c)] Gian Luigi Bendazzoli,[4,d)] Stefano Evangelisti,[1,e)] and Thierry Leininger[1,f)]

[1]*Laboratoire de Chimie et Physique Quantiques - LCPQ/IRSAMC, Université de Toulouse (UPS) et CNRS (UMR-5626), 118, Route de Narbonne, 31062 Toulouse Cedex, France*
[2]*Departamento de Química, Facultad de Ciencias, Módulo 13, Universidad Autónoma de Madrid, Cantoblanco, 28049 Madrid, Spain*
[3]*Institut für Chemie und Biochemie - Physikalische und Theoretische Chemie, Freie Universität Berlin, Takustr. 3, D-14195 Berlin, Germany*
[4]*Dipartimento di Chimica Industriale "Toso Montanari", Università di Bologna, Viale Risorgimento 4, I–40136 Bologna, Italy*

The Total Position Spread (TPS) tensor, defined as the second moment cumulant of the position operator, is a key quantity to describe the mobility of electrons in a molecule or an extended system. In the present investigation, the partition of the TPS tensor according to spin variables is derived and discussed. It is shown that, while the spin-summed TPS gives information on charge mobility, the spin-partitioned TPS tensor becomes a powerful tool that provides information about spin fluctuations. The case of the hydrogen molecule is treated, both analytically, by using a $1s$ Slater-type orbital, and numerically, at Full Configuration Interaction (FCI) level with a V6Z basis set. It is found that, for very large inter-nuclear distances, the partitioned tensor growths quadratically with the distance in some of the low-lying electronic states. This fact is related to the presence of entanglement in the wave function. Non-dimerized open chains described by a model Hubbard Hamiltonian and linear hydrogen chains H_n ($n \geq 2$), composed of equally spaced atoms, are also studied at FCI level. The hydrogen systems show the presence of marked maxima for the spin-summed TPS (corresponding to a high charge mobility) when the inter-nuclear distance is about 2 bohrs. This fact can be associated to the presence of a Mott transition occurring in this region. The spin-partitioned TPS tensor, on the other hand, has a quadratical growth at long distances, a fact that corresponds to the high spin mobility in a magnetic system. © 2015 AIP Publishing LLC. [http://dx.doi.org/10.1063/1.4913734]

I. INTRODUCTION

The Localization tensor (LT) and Total-Position Spread (TPS) tensor are quantities stemming from Kohn's theory[1] of electrical conductivity. Indeed, in his seminal work, Kohn argued that the fundamental nature of electrical conductivity is more related to a properly defined delocalization of the wave function than to the simple gap closure. Subsequently, Resta and coworkers introduced the LT and provided an important tool to give a quantitative formulation of this localization.[2–6] Later, a remarkable sum rule, connecting explicitly electrical resistivity and localization tensor, was given by Souza and Wilkens.[7] According to these results, the key property of this quantity is the following: *the Localization Tensor diverges in the thermodynamic limit for a conductor, while remaining finite for an insulator.*[8,9]

In recent years, our group has been investigating the properties of what we named the TPS tensor, $\mathbf{\Lambda}$.[10] Notice that LT

and TPS are trivially related, since the original LT introduced by Resta is nothing but our TPS tensor divided by the number of electrons. In our investigation, we considered several structures (atoms, molecules, clusters), treated either by *ab initio*,[11–14] or *model*[15,16] Hamiltonians. Although essentially equivalent quantities, we believe that, in a molecular context, the TPS tensor is more pertinent than the LT.[10,17,18] In fact, in this context, it is useful to have a property like TPS that is strongly dependent upon the number of electrons or the size of the system, in order to follow processes like chemical reactions or fragmentation. Moreover, the contribution of the different electronic shells to the TPS is extremely inhomogeneous, so performing an average on these different terms has little meaning. We notice, however that the use of the LT can be advantageous in some other cases, particularly when the asymptotic dependence upon the size of the system is studied.

We found the TPS tensor is a useful and powerful tool to provide information about metal-insulator transitions, by computing it for finite systems of increasing size.[12,19–22] In such a way, its asymptotic behavior can be investigated. Moreover we computed the TPS tensor for several molecular systems and found that it is capable of detecting other types of transitions, like charge transfer, bond formation/breaking, and other processes related to the mobility of the electrons.[10,14,23]

a)elkhatib@irsamc.ups-tlse.fr
b)oriana.brea@uam.es
c)edoardo.fertitta@fu-berlin.de.
d)gianluigi.bendazzoli@unibo.it
e)stefano@irsamc.ups-tlse.fr
f)Thierry.Leininger@irsamc.ups-tlse.fr

In the present work, the partition of the TPS tensor according to its spin components is presented and discussed. It is shown that the different spin components of the TPS tensor give important information about the behavior of the electrons in molecular systems, in particular about spin-dependent properties. The formalism is illustrated through applications to the hydrogen dimer and one-dimensional model systems. The case of the hydrogen dimer ($n = 2$) is particularly useful to get some insight into the structure of the TPS, and it is discussed in detail in this work. Indeed, by using a basis set of a single $1s$ Slater-Type Orbital (STO) per atom, a complete analytical treatment of the TPS is possible for H_2. All the integrals involved in the matrix elements of the Hamiltonian operator as well as the TPS tensor $\mathbf{\Lambda}$ can be analytically evaluated.[24,25] In this way, the different terms that appear in the expressions of the perpendicular and parallel components, $\Lambda^\perp$ and $\Lambda^\parallel$, respectively, can be calculated at any inter-nuclear distance R. It will also be shown that the asymptotic behavior at large R of $\Lambda^\parallel$ is related to the presence of *entanglement* in the wave function.[26,27] Notice that this analytical solution has not only an intrinsic interest but can be particularly useful as a benchmark result in order to test approximate methods or numerical approaches.

For the low-lying states of the hydrogen dimer, the spin-summed and spin-partitioned spread tensors are also numerically computed at the full configuration interaction (FCI) level, by using a large basis set of sextuple-zeta quality. Indeed, while at large inter-atomic distance, the STO basis set gives the exact result for the neutral states, the presence of dynamical correlation implies that large basis sets are needed in order to obtain quantitatively correct results at short inter-nuclear distances and for the ionic states.

As far as model Hamiltonians are concerned, we investigated the behavior of non-dimerized chains of two different types:

- open chains described by a Hubbard Hamiltonian, Hub_n;
- linear chains of hydrogen atoms, H_n.

Dimerized hydrogen chains show a range of different behaviors, depending on the type of dimerization. They have been the object of a separate investigation.[28] The case of Hubbard open chains has been numerically investigated at FCI level. These chains are extremely well studied systems, both analytically and numerically.[29–36] They have a behavior going from highly correlated magnetic systems, when the intra-site repulsion U is large with respect to the hopping integral t, to uncorrelated systems of Hückel type in the opposite limit. The numerical study shows that both the Spin-Summed and Spin-Partitioned TPS (SS-TPS and SP-TPS, respectively) tensors clearly reflect this type of behaviors.

As concerns hydrogen chains H_n for $n \geq 2$, the calculations were performed at FCI level with a $1s$ STO orbital per atom, for even values of n going from two to sixteen and for equally spaced atoms. In our previous works on this subject, it has been shown that the TPS tensor presents a maximum at an inter-atomic separation of about 2 bohrs. For larger values of the distance, the tensor goes down to n times the atomic value, as one expects from an additive quantity. The value of the maximum, however, grows *faster than linearly*

as a function of the number of atoms n. This fact suggests the presence of a Metal-Insulator Transition (MIT)[37] at this distance.[19,21] Indeed, hydrogen chains are often viewed as paradigmatic systems for describing Mott transitions.[22,38–43] The behavior of the spin-partitioned tensor, on the other hand, is completely different, since both the equal-spin and different-spin components diverge for large distance, the two terms having opposite signs. This is related to the fact that non-dimerized hydrogen chains become highly correlated magnetic systems in the insulator regime. These results show that, while the spin-summed spread tensor gives information on the charge mobility, regardless their spin components, the spin-partitioned tensor gives analogous information on the spin mobility, and the propagation of magnetic modes in particular.

This article is organized in the following way: in Sec. II, the formalism of the spin-partitioned TPS tensor is developed and in Sec. II C, the particular case of a single Slater determinant is given. In Sec. III, the analytical treatment of the hydrogen dimer is performed and discussed. Section IV A describes the computational details employed in this investigation, while in Sec. IV B, H_2 is treated at FCI level. Numerical full CI computations concerning Hubbard and hydrogen chains are presented in Secs. IV C and IV D, respectively. Finally, in Sec. V, some conclusions are drawn, and plans for future works on the subject are given.

II. THE SPIN PARTITION OF THE TPS TENSOR

We describe in this section the decomposition of the $\mathbf{\Lambda}$ tensor accordingly to the spin variables.

A. Some formal properties

The second cumulant[44] $\bar{\bar{\mathbf{A}}}$ of a generic vector operator $\hat{\mathbf{A}}$ is a tensor of rank two, defined as

$$\bar{\bar{\mathbf{A}}} = \langle\Psi|\hat{\mathbf{A}}^2|\Psi\rangle - \langle\Psi|\hat{\mathbf{A}}|\Psi\rangle^2 = \langle\Psi|\hat{\mathbf{A}}^2|\Psi\rangle - \bar{\mathbf{A}}^2, \quad (1)$$

where we have defined $\bar{\mathbf{A}} = \langle\Psi|\hat{\mathbf{A}}|\Psi\rangle$. This is equivalent to writing

$$\bar{\bar{\mathbf{A}}} = \langle\Psi|(\hat{\mathbf{A}} - \bar{\mathbf{A}})^2|\Psi\rangle. \quad (2)$$

From this last equation, it is clear that $\bar{\bar{\mathbf{A}}}$ is manifestly definite positive. It is also invariant with respect to a coordinate translation $\hat{\mathbf{A}} \to \hat{\mathbf{A}} + \mathbf{a}$ because, under such a transformation, $\bar{\mathbf{A}} \to \bar{\mathbf{A}} + \mathbf{a}$.

We consider now the case of an operator $\hat{\mathbf{C}}$ which is the sum of two operators, $\hat{\mathbf{C}} = \hat{\mathbf{A}} + \hat{\mathbf{B}}$. As concerns the mean values, we trivially have

$$\bar{\mathbf{C}} = \bar{\mathbf{A}} + \bar{\mathbf{B}}. \quad (3)$$

On the other hand, the cumulant $\bar{\bar{\mathbf{C}}}$ of $\hat{\mathbf{C}}$ becomes

$$\begin{aligned}
\bar{\bar{\mathbf{C}}} &= \langle\Psi|(\hat{\mathbf{A}} + \hat{\mathbf{B}})^2|\Psi\rangle - (\bar{\mathbf{A}} + \bar{\mathbf{B}})^2 \\
&= \langle\Psi|\hat{\mathbf{A}}^2|\Psi\rangle + \langle\Psi|\hat{\mathbf{B}}^2|\Psi\rangle \\
&\quad + \langle\Psi|\hat{\mathbf{A}}\hat{\mathbf{B}}|\Psi\rangle + \langle\Psi|\hat{\mathbf{B}}\hat{\mathbf{A}}|\Psi\rangle \\
&\quad - (\langle\bar{\mathbf{A}}\rangle^2 + \langle\bar{\mathbf{B}}\rangle^2 + 2\hat{\mathbf{A}}\hat{\mathbf{B}}) \\
&= \bar{\bar{\mathbf{A}}} + \bar{\bar{\mathbf{B}}} + \langle\Psi|\hat{\mathbf{A}}\hat{\mathbf{B}} + \hat{\mathbf{B}}\hat{\mathbf{A}}|\Psi\rangle - 2\bar{\mathbf{A}}\bar{\mathbf{B}}. \quad (4)
\end{aligned}$$

Therefore, the cumulant of $\hat{\mathbf{C}}$ is not the sum of the cumulants of the operators $\hat{\mathbf{A}}$ and $\hat{\mathbf{B}}$, due to the presence of the mixed additional terms

$$\langle\Psi|\hat{\mathbf{A}}\hat{\mathbf{B}} + \hat{\mathbf{B}}\hat{\mathbf{A}}|\Psi\rangle - 2\,\bar{\mathbf{A}}\bar{\mathbf{B}}. \tag{5}$$

However there is an important case where this additional term is zero, namely, when a system separates into fragments (see the Appendix on size additivity).

In Subsection II B, the case of the total-position operator is considered. It can be expressed as the sum of two spin parts, α and β, and it turns out that its second cumulant becomes the sum of three terms: the $\alpha\alpha$ and $\beta\beta$ cumulants, plus a mixed $\alpha\beta$ term. This is the central point of the SP-TPS tensor presented in this article.

B. General spin-partition formalism

In order to do the spin partition of the TPS tensor, the position operator $\hat{\mathbf{r}}$ is expressed as the sum of its spin components. As far as the spin is concerned, we indicate by the subscript σ a generic spin component, either α or β. Then, one can write

$$\hat{\mathbf{r}} = \sum_{\sigma=\alpha,\beta} \hat{\mathbf{r}}_\sigma, \tag{6}$$

where $\hat{\mathbf{r}}$ has Cartesian components $\hat{r}_x$, $\hat{r}_y$, and $\hat{r}_z$. From the one-particle position operator $\hat{\mathbf{r}}$, it is possible to define the total position operator $\hat{\mathbf{R}}$ for a system of n particles as

$$\hat{\mathbf{R}} = \sum_{i=1}^n \sum_{\sigma=\alpha,\beta} \hat{\mathbf{r}}_\sigma(i). \tag{7}$$

The TPS tensor is defined as the second moment cumulant of the total position operator,

$$\mathbf{\Lambda} = \langle\Psi|\hat{\mathbf{R}}^2|\Psi\rangle - \langle\Psi|\hat{\mathbf{R}}|\Psi\rangle^2. \tag{8}$$

Since the tensor $\mathbf{\Lambda}$ does not depend on the origin of the coordinate system, it can be conveniently computed in the particular coordinate system where $\langle\hat{R}\rangle = 0$, because in that case, we simply have

$$\mathbf{\Lambda} = \langle\Psi|\hat{\mathbf{R}}^2|\Psi\rangle \qquad (\langle\Psi|\hat{\mathbf{R}}|\Psi\rangle = 0). \tag{9}$$

Since the operator $\hat{\mathbf{R}}$ can be expressed as the sum of *two* parts, an α and a β one, the squared operator $\hat{R}^2$ becomes the sum of *four* terms: $\alpha\alpha$, $\alpha\beta$, $\beta\alpha$, and $\beta\beta$. Therefore, we have

$$\hat{\mathbf{R}} = \hat{\mathbf{R}}_\alpha + \hat{\mathbf{R}}_\beta \tag{10}$$

and

$$\hat{\mathbf{R}}^2 = \hat{\mathbf{R}}_\alpha^2 + \hat{\mathbf{R}}_\beta^2 + \hat{\mathbf{R}}_\alpha\hat{\mathbf{R}}_\beta + \hat{\mathbf{R}}_\beta\hat{\mathbf{R}}_\alpha. \tag{11}$$

In this way, also the TPS tensor $\mathbf{\Lambda}$ decomposes in the sum of four different terms

$$\mathbf{\Lambda}_{\alpha\alpha} = \langle\Psi|\hat{\mathbf{R}}_\alpha^2|\Psi\rangle - \langle\Psi|\hat{\mathbf{R}}_\alpha|\Psi\rangle^2, \tag{12}$$

$$\mathbf{\Lambda}_{\beta\beta} = \langle\Psi|\hat{\mathbf{R}}_\beta^2|\Psi\rangle - \langle\Psi|\hat{\mathbf{R}}_\beta|\Psi\rangle^2, \tag{13}$$

$$\mathbf{\Lambda}_{\alpha\beta} = \langle\Psi|\hat{\mathbf{R}}_\alpha\hat{\mathbf{R}}_\beta|\Psi\rangle - \langle\Psi|\hat{\mathbf{R}}_\alpha|\Psi\rangle\langle\Psi|\hat{\mathbf{R}}_\beta|\Psi\rangle, \tag{14}$$

$$\mathbf{\Lambda}_{\beta\alpha} = \langle\Psi|\hat{\mathbf{R}}_\beta\hat{\mathbf{R}}_\alpha|\Psi\rangle - \langle\Psi|\hat{\mathbf{R}}_\beta|\Psi\rangle\langle\Psi|\hat{\mathbf{R}}_\alpha|\Psi\rangle. \tag{15}$$

Notice, however, that $\mathbf{\Lambda}_{\alpha\beta}$ and $\mathbf{\Lambda}_{\beta\alpha}$ cannot be distinguished, because the commutator between $\hat{\mathbf{R}}_\alpha$ and $\hat{\mathbf{R}}_\beta$ vanishes. Moreover, for wave functions having the $\bar{S}_z$ spin component equal to zero, $\mathbf{\Lambda}_{\alpha\alpha}$ and $\mathbf{\Lambda}_{\beta\beta}$ are identical. For this reason, we will report in this work the global component $\mathbf{\Lambda}_{\alpha\beta+\beta\alpha}$ and, in all cases where $S_z = 0$, the sum of the two components, $\mathbf{\Lambda}_{\alpha\alpha}$ and $\mathbf{\Lambda}_{\beta\beta}$, indicated as $\mathbf{\Lambda}_{\alpha\alpha+\beta\beta}$. It is worth to stress the fact that $\mathbf{\Lambda}_{\alpha\alpha}$ and $\mathbf{\Lambda}_{\beta\beta}$ are second-order cumulants themselves, of the spin-projected total-position operators $\hat{\mathbf{R}}_\alpha$ and $\hat{\mathbf{R}}_\beta$, and, satisfy, therefore all the corresponding properties (their sum, however, *is not* a cumulant). The quantities $\mathbf{\Lambda}_{\alpha\beta}$ and $\mathbf{\Lambda}_{\beta\alpha}$, on the other hand, are joint cumulants,[45,46] and they are not necessarily positive definite. The SS-TPS can be seen as the sum of joint cumulants where those involving identical random variables are the variance, and those of two random variables are the covariance that can have a negative value as well. This fact will be illustrated, for instance, in the section on applications, where it will be seen that $\mathbf{\Lambda}_{\alpha\alpha}$ and $\mathbf{\Lambda}_{\beta\beta}$ are always positive, while $\mathbf{\Lambda}_{\alpha\beta} + \mathbf{\Lambda}_{\beta\alpha}$ does not have a definite sign.

The complete, SS-TPS tensor is given by

$$\mathbf{\Lambda} = \mathbf{\Lambda}_{\alpha\alpha} + \mathbf{\Lambda}_{\beta\beta} + \mathbf{\Lambda}_{\alpha\beta} + \mathbf{\Lambda}_{\beta\alpha} = \mathbf{\Lambda}_{\alpha\alpha+\beta\beta} + \mathbf{\Lambda}_{\alpha\beta+\beta\alpha}. \tag{16}$$

If $\langle\Psi|\hat{\mathbf{R}}_\alpha|\Psi\rangle = 0$, we have

$$\mathbf{\Lambda}_{\alpha\alpha} = \langle\Psi|\hat{\mathbf{R}}_\alpha^2|\Psi\rangle \qquad (\langle\Psi|\hat{\mathbf{R}}_\alpha|\Psi\rangle = 0) \tag{17}$$

and

$$\mathbf{\Lambda}_{\alpha\beta+\beta\alpha} = \langle\Psi|\hat{\mathbf{R}}_\alpha\hat{\mathbf{R}}_\beta|\Psi\rangle \qquad (\langle\Psi|\hat{\mathbf{R}}_\alpha|\Psi\rangle = 0), \tag{18}$$

while if it is $\langle\Psi|\hat{\mathbf{R}}_\beta|\Psi\rangle = 0$, we have

$$\mathbf{\Lambda}_{\beta\beta} = \langle\Psi|\hat{\mathbf{R}}_\beta^2|\Psi\rangle \qquad (\langle\Psi|\hat{\mathbf{R}}_\beta|\Psi\rangle = 0) \tag{19}$$

and

$$\mathbf{\Lambda}_{\alpha\beta+\beta\alpha} = \langle\Psi|\hat{\mathbf{R}}_\alpha\hat{\mathbf{R}}_\beta|\Psi\rangle \qquad (\langle\Psi|\hat{\mathbf{R}}_\beta|\Psi\rangle = 0). \tag{20}$$

Notice that $\langle\Psi|\hat{\mathbf{R}}|\Psi\rangle = \langle\Psi|\hat{\mathbf{R}}_\alpha|\Psi\rangle + \langle\Psi|\hat{\mathbf{R}}_\beta|\Psi\rangle$. However, in general, $\langle\Psi|\hat{\mathbf{R}}_\alpha|\Psi\rangle$ and $\langle\Psi|\hat{\mathbf{R}}_\beta|\Psi\rangle$ will be different. Therefore, by a suitable coordinate translation, it is not possible to annihilate simultaneously both $\langle\Psi|\hat{\mathbf{R}}_\alpha|\Psi\rangle$ and $\langle\Psi|\hat{\mathbf{R}}_\beta|\Psi\rangle$. Hence, normally one can not express the different TPS spin contributions via Eqs. (17)–(20). In particular, if the coordinates are chosen in such a way that $\langle\Psi|\hat{\mathbf{R}}|\Psi\rangle = 0$ (and therefore $\langle\Psi|\hat{\mathbf{R}}_\alpha|\Psi\rangle = -\langle\Psi|\hat{\mathbf{R}}_\beta|\Psi\rangle$), the SS-TPS will be given by Eq. (9), but Eqs. (17)–(20) will not hold. It is only when $\langle\Psi|\hat{\mathbf{R}}_\alpha|\Psi\rangle = \langle\Psi|\hat{\mathbf{R}}_\beta|\Psi\rangle$ that Eqs. (6)–(17) can simultaneously hold. In fact, in such a case, by a suitable coordinate translation, we can have both $\langle\Psi|\hat{\mathbf{R}}_\alpha|\Psi\rangle = 0$ and $\langle\Psi|\hat{\mathbf{R}}_\beta|\Psi\rangle = 0$, and therefore $\langle\Psi|\hat{\mathbf{R}}|\Psi\rangle = \langle\Psi|\hat{\mathbf{R}}_\alpha|\Psi\rangle + \langle\Psi|\hat{\mathbf{R}}_\beta|\Psi\rangle = 0$.

C. Single-determinant case

If the wave function can be expressed by a single Slater determinant, $|\Phi_0\rangle$, the mixed identically components vanish. Indeed, by inserting a resolution of the identity $\sum_I |\Phi_I\rangle\langle\Phi_I|$ between the two $\hat{\mathbf{R}}$ operators in $\hat{\mathbf{R}}^2$, we have

$$\langle\Phi_0|\hat{\mathbf{R}}^2|\Phi_0\rangle = \sum_I \langle\Phi_0|\hat{\mathbf{R}}|\Phi_I\rangle\langle\Phi_I|\hat{\mathbf{R}}|\Phi_0\rangle. \tag{21}$$

Since $\hat{\mathbf{R}}$ is a one-electron operator, the determinant $|\Phi_I\rangle$ in Eq. (21) is either $|\Phi_0\rangle$ itself or a single excitation $|\Phi_{I_1}\rangle$ from

the determinant $|\Phi_0\rangle$. But a single excitation $|\Phi_{I_1}\rangle$ cannot be simultaneously an α and a β excitation from $|\Phi_0\rangle$, hence

$$\langle\Phi_0|\hat{\mathbf{R}}_\alpha|\Phi_{I_1}\rangle\langle\Phi_{I_1}|\hat{\mathbf{R}}_\beta|\Phi_0\rangle = 0. \qquad (22)$$

This means that the single $\alpha\beta$ and $\beta\alpha$ contributions vanish

$$\sum_{I_1}\langle\Phi_0|\hat{\mathbf{R}}_\alpha|\Phi_{I_1}\rangle\langle\Phi_{I_1}|\hat{\mathbf{R}}_\beta|\Phi_0\rangle$$
$$= \sum_{I_1}\langle\Phi_0|\hat{\mathbf{R}}_\beta|\Phi_{I_1}\rangle\langle\Phi_{I_1}|\hat{\mathbf{R}}_\alpha|\Phi_0\rangle = 0. \qquad (23)$$

The only surviving term in the resolution of the identity, Eq. (21), is when $|\Phi_I\rangle = |\Phi_0\rangle$. This means that

$$\langle\Phi_0|\hat{\mathbf{R}}_\alpha\hat{\mathbf{R}}_\beta|\Phi_0\rangle = \langle\Phi_0|\hat{\mathbf{R}}_\alpha|\Phi_0\rangle\langle\Phi_0|\hat{\mathbf{R}}_\beta|\Phi_0\rangle \qquad (24)$$

and hence $\Lambda_{\alpha\beta} = 0$ (see Eq. (14)). The same result holds obviously for $\Lambda_{\beta\alpha}$.

III. THE HYDROGEN DIMER: ANALYTICAL TREATMENT

The case of a hydrogen molecule described by a STO minimal basis set will be considered in this section. It is an instructive system admitting an analytical solution. Although more general expressions can be obtained by using generic localized orbitals, the STO result has the important advantage of representing a useful benchmark in order to validate numerical treatments.

We consider two hydrogen nuclei, located in the two points $A(0, 0, -R/2)$ and $B(0, 0, R/2)$, with a $1s$ STO orbital on each of them. All the integrals needed to calculate Λ for this simple system can be analytically evaluated (see Ref. 47 and references therein). The two normalized atomic orbitals $1s_A$ and $1s_B$ are located in A and B, respectively; they are functions of the vector $\mathbf{r}$ with Cartesian components x, y, z and give rise to two normalized molecular orbitals σ_g and σ_u

$$\sigma_g = \frac{1s_A + 1s_B}{\sqrt{2 + 2S_{AB}}}, \quad \text{and} \quad \sigma_u = \frac{1s_A - 1s_B}{\sqrt{2 - 2S_{AB}}},$$

where S_{AB} is the two-center overlap integral. In order to simplify the notation, we will use the symbols A, B and g, u to denote these atomic and molecular orbitals, respectively. A Slater determinant will be denoted by an ordered product of spin-orbitals, possibly enclosed in $|\cdots\rangle$; a simple orbital symbol like g will be understood to have α spin, while the corresponding β spin-orbital will be denoted by $\bar{g}$. There are six possible Slater determinants: $|g\bar{g}\rangle$ and $|u\bar{u}\rangle$ have symmetry $^1\Sigma_g^+$, $|g\bar{u}\rangle$ and $|\bar{g}u\rangle$ have symmetry Σ_u^+ and originate a singlet and a triplet state, while $|gu\rangle$, $|\bar{g}\bar{u}\rangle$ are the $S_z = \pm 1$ components of a $^3\Sigma_u^+$ state. Four states can be generated by using this minimal basis set. They are two symmetric singlets,

$$|1^1\Sigma_g^+\rangle = \cos\theta\,|g\bar{g}\rangle + \sin\theta\,|u\bar{u}\rangle, \qquad (25)$$

$$|2^1\Sigma_g^+\rangle = \sin\theta\,|g\bar{g}\rangle - \cos\theta\,|u\bar{u}\rangle \qquad (26)$$

(where θ is a variational parameter), an antisymmetric singlet,

$$|^1\Sigma_u^+\rangle = \frac{|g\bar{u}\rangle - |\bar{g}u\rangle}{\sqrt{2}} \qquad (27)$$

and an antisymmetric triplet, whose three components are

$$|^{3(+1)}\Sigma_u^+\rangle = |gu\rangle, \qquad (28)$$

$$|^{3(0)}\Sigma_u^+\rangle = \frac{|g\bar{u}\rangle + |\bar{g}u\rangle}{\sqrt{2}}, \qquad (29)$$

$$|^{3(-1)}\Sigma_u^+\rangle = |\bar{g}\bar{u}\rangle. \qquad (30)$$

In Sec. III A, we compute the matrix elements of the required operators on the g, u and the determinantal basis set. Then, in Sec. III B, the mean values of the same operators on the basis of the Hamiltonian eigenfunctions are calculated. Finally, in Sec. III C, the behavior of the TPS tensor at large distances is computed and discussed.

A. Matrix elements

We consider now the case of the longitudinal (zz or $\parallel$) component of the TPS tensor. Since the transversal (xx, yy or $\perp$) component does show a less spectacular behavior, its derivation will not be reported here, but it can be found in the supplementary material.[48] We denote by $\hat{z}$, $\hat{z}^2$ the longitudinal components of the vector operator $\hat{\mathbf{R}}$, $\hat{\mathbf{R}}^2$, respectively.

By taking into account the Eqs. (A1)–(A6) displayed in Subsection 1 of the Appendix, matrix elements of the z^2 operator are defined as

$$\langle A_\sigma(i)X_{\bar{\sigma}}(j)|\hat{z}_\sigma^2(i)|A_\sigma(i)X_{\bar{\sigma}}(j)\rangle = \frac{R^2}{4} + \frac{1}{Z^2}, \qquad (31)$$

where $X = A$, B and Z = nuclear charge, while

$$\langle A_\sigma(i)B_{\bar{\sigma}}(j)|\hat{z}_\sigma^2(i)|B_\sigma(i)A_{\bar{\sigma}}(j)\rangle = s_{AB}\,z_{AB}^2 \qquad (32)$$

and the overlap s_{AB} and z_{AB}^2 are functions of R given in the Appendix.

In Table I, the matrix elements on the determinant basis are shown (the derivation of matrix elements on the MO basis can be found in the supplementary material[48]). As expected from Sec. II C, the $\alpha\alpha + \beta\beta$ contributions are the only non-vanishing ones for the $|g\bar{g}\rangle$ and $|u\bar{u}\rangle$ determinants

$$\Lambda_{\alpha\alpha+\beta\beta}^{\parallel}(|g\bar{g}\rangle) = \frac{2}{1+s_{AB}}\left(\frac{1}{Z^2} + \frac{R^2}{4} + z_{AB}^2\right) \qquad (33)$$

and

$$\Lambda_{\alpha\alpha+\beta\beta}^{\parallel}(|u\bar{u}\rangle) = \frac{2}{1-s_{AB}}\left(\frac{1}{Z^2} + \frac{R^2}{4} - z_{AB}^2\right) \qquad (34)$$

while

$$\Lambda_{\alpha\beta+\beta\alpha}^{\parallel}(|g\bar{g}\rangle) = \Lambda_{\alpha\beta+\beta\alpha}^{\parallel}(|u\bar{u}\rangle) = 0. \qquad (35)$$

B. The spreads for the different states

As a preliminary result, the TPS tensor will be computed for the hydrogen atom. For a neutral hydrogen atom, one has

$$\Lambda^{\parallel}(|1s\rangle) = \Lambda^{\perp}(|1s\rangle) = \frac{1}{Z^2} = 1. \qquad (36)$$

Equation (36) can be written in a compact form as $\Lambda(|1s\rangle) = 1$. The anion is described, at a single STO level, by a closed-shell determinant. This implies that the position spread is

TABLE I. Matrix elements between Slater determinants of the hydrogen dimer in the determinant basis.

Determinant symmetry	Matrix elements
Σ_g^+	$\langle g\bar{g}|\hat{z}^2|g\bar{g}\rangle = \frac{2}{1+s_{AB}}\left(\frac{1}{Z^2} + \frac{R^2}{4} + z_{AB}^2\right)$
	$\langle u\bar{u}|\hat{z}^2|u\bar{u}\rangle = \frac{2}{1-s_{AB}}\left(\frac{1}{Z^2} + \frac{R^2}{4} - z_{AB}^2\right)$
	$\langle g\bar{g}|\hat{z}^2|u\bar{u}\rangle = \frac{R^2}{2(1-s_{AB}^2)}$
Σ_u^+	$\langle g\bar{u}|\hat{z}^2|g\bar{u}\rangle = \frac{2}{1-s_{AB}^2}\left(\frac{1}{Z^2} + \frac{R^2}{4} - s_{AB}^2 z_{AB}^2\right)$
	$\langle g\bar{u}|\hat{z}^2|\bar{g}u\rangle = -\frac{R^2}{2(1-s_{AB}^2)}$
	$\langle gu|\hat{z}^2|gu\rangle = \langle \bar{g}\bar{u}|\hat{z}^2|\bar{g}\bar{u}\rangle = \frac{2}{2(1-s_{AB}^2)}\left(\frac{1}{Z^2} + s_{AB}z_{AB}^2 + \frac{R^2}{2}\right)$

additive on the two electron components, and therefore one has

$$\Lambda(|1s^2\rangle) = \frac{2}{Z^2} = 2. \qquad (37)$$

Notice, however, that because of the lack of correlation, the hydrogen anion is unstable with respect to an auto-ionization process if the system is described by a minimal basis set.

The TPS tensor for H_2^{2+} is trivially zero. In the case of the H_2^+ molecule, two states are possible within the minimal basis-set description: the ground state symmetric doublet $^2\Sigma_g^+$ and the excited antisymmetric doublet $^2\Sigma_u^+$. They are obtained by placing a single electron (either an α or a β one) in the g or u orbital, respectively. The total spread coincides with either the $\alpha\alpha$ or the $\beta\beta$ components, depending on the spin projection of the electron. One obtains

$$\Lambda^{\parallel}(|^2\Sigma_g^+\rangle) = \langle g|z^2|g\rangle$$
$$= \frac{1}{1+s_{AB}}\left(\frac{1}{Z^2} + \frac{R^2}{4} + z_{AB}^2\right) \qquad (38)$$

and

$$\Lambda^{\parallel}(|^2\Sigma_u^+\rangle) = \langle u|z^2|u\rangle$$
$$= \frac{1}{1-s_{AB}}\left(\frac{1}{Z^2} + \frac{R^2}{4} - z_{AB}^2\right). \qquad (39)$$

We now compute the spin-contributions of the TPS tensor for the different states of the hydrogen dimer described by a minimal basis set: for the two θ-dependent symmetric singlets, the $^1\Sigma_g^+$ states, we have

$$\Lambda^{\parallel}_{\alpha\alpha+\beta\beta}(|^1\Sigma_g^+(\theta)\rangle) = \frac{2\cos^2\theta}{1+s_{AB}}\left(\frac{1}{Z^2} + \frac{R^2}{4} + z_{AB}^2\right)$$
$$+ \frac{2\sin^2\theta}{1-s_{AB}}\left(\frac{1}{Z^2} + \frac{R^2}{4} - z_{AB}^2\right) \qquad (40)$$

and

$$\Lambda^{\parallel}_{\alpha\beta+\beta\alpha}(|^1\Sigma_g^+(\theta)\rangle) = 2\frac{\cos\theta\sin\theta}{(1-s_{AB}^2)}\frac{R^2}{2}. \qquad (41)$$

In a similar way, for the antisymmetric singlet $^1\Sigma_u^+$ state, we have

$$\Lambda^{\parallel}_{\alpha\alpha+\beta\beta}(|^1\Sigma_u^+\rangle) = \langle g|z^2|g\rangle + \langle u|z^2|u\rangle$$
$$= \frac{1}{1+s_{AB}}\left(\frac{1}{Z^2} + \frac{R^2}{4} + z_{AB}^2\right)$$
$$+ \frac{1}{1-s_{AB}}\left(\frac{1}{Z^2} + \frac{R^2}{4} - z_{AB}^2\right) \qquad (42)$$

and

$$\Lambda^{\parallel}_{\alpha\beta+\beta\alpha}(|^1\Sigma_u^+\rangle) = -\langle g\bar{u}|z^2|\bar{g}u\rangle = 2\langle g|z|u\rangle^2$$
$$= \frac{1}{(1-s_{AB}^2)}\frac{R^2}{2}. \qquad (43)$$

We consider now the antisymmetric triplet $^3\Sigma_u^+$ state. For the $S_z = 0$ component, $^{3(0)}\Sigma_u^+$, we have

$$\Lambda^{\parallel}_{\alpha\alpha+\beta\beta}(|^{3(0)}\Sigma_u^+\rangle) = \langle g|z^2|g\rangle + \langle u|z^2|u\rangle$$
$$= \frac{1}{1+s_{AB}}\left(\frac{1}{Z^2} + \frac{R^2}{4} + z_{AB}^2\right)$$
$$+ \frac{1}{1-s_{AB}}\left(\frac{1}{Z^2} + \frac{R^2}{4} - z_{AB}^2\right) \qquad (44)$$

and

$$\Lambda^{\parallel}_{\alpha\beta+\beta\alpha}(|^{3(0)}\Sigma_u^+\rangle) = -2\langle g|z|u\rangle^2$$
$$= -\frac{1}{(1-s_{AB}^2)}\frac{R^2}{2}. \qquad (45)$$

For the other components, $^{3(\pm1)}\Sigma_u^+$, only the $\Lambda_{\alpha\alpha}$ and $\Lambda_{\beta\beta}$ components, respectively, will be different from zero

$$\Lambda^{\parallel}_{\alpha\alpha}(^{3(1)}\Sigma_u^+) = \Lambda^{\parallel}_{\beta\beta}(^{3(-1)}\Sigma_u^+)$$
$$= \langle g|z^2|g\rangle + \langle u|z^2|u\rangle - 2\langle g|z|u\rangle^2$$
$$= \frac{1}{1+s_{AB}}\left(\frac{1}{Z^2} + \frac{R^2}{4} + z_{AB}^2\right)$$
$$+ \frac{1}{1-s_{AB}}\left(\frac{1}{Z^2} + \frac{R^2}{4} - z_{AB}^2\right)$$
$$- \frac{1}{(1-s_{AB}^2)}\frac{R^2}{2}. \qquad (46)$$

TABLE II. The isolated-atom and long-distance asymptotic values of energy and TPS tensor, parallel components, for some hydrogen systems. The quadratically divergent R^2 terms are due to the presence of entanglement in the wave function. With this basis set, the energy of the hydrogen atom and anion, $E(H)$ and $E(H^-)$, respectively, is given by $E(H) = -0.500\,000\,00$ and $E(H^-) = -0.375\,000\,27$. Notice that the anion is not stable with respect to auto-ionization. All numerical values in atomic units.

System	Electrons	E	$\Lambda^\parallel$	$\Lambda^\parallel_{\alpha\alpha+\beta\beta}$	Electronic state
H^+	0	0	0	0	$\cdots$
H	1	$E(H)$	1	1	$^2S_{1/2}$
H^-	2	$E(H^-)$	2	2	$^1S_0$
$H \cdots H^+$	1	$E(H)$	1	1	
$H \cdots H^+ \pm H^+ \cdots H$	1	$E(H)$	$1 + R^2/4$	$1 + R^2/4$	$^2\Sigma_g^+, {}^2\Sigma_u^+$
$H \cdots \bar{H}$	2	$2E(H)$	2	2	
$H \cdots \bar{H} \pm \bar{H} \cdots H$	2	$2E(H)$	2	$2 + R^2/2$	$1^1\Sigma_g^+, {}^3\Sigma_u^+$
$H \cdots H ; \bar{H} \cdots \bar{H}$	2	$2E(H)$	2	2	$^3\Sigma_u^+$
$H^+ \cdots H^-$	2	$E(H^-)$	2	2	
$H^+ \cdots H^- \pm H^- \cdots H^+$	2	$E(H^-)$	$2 + R^2$	$2 + R^2/2$	$1\Sigma_u^+, 2^1\Sigma_g^+$
$H \cdots H^-$	3	$E(H) + E(H^-)$	3	3	
$H \cdots H^- \pm H^- \cdots H$	3	$E(H) + E(H^-)$	$3 + R^2/4$	$3 + R^2/4$	$^2\Sigma_g^+, {}^2\Sigma_u^+$

C. The asymptotic behavior: Wave function entanglement

It is useful to consider the long-distance behavior of the longitudinal components of the TPS tensor for the different states. In fact, the asymptotic value of the TPS tensor is related to the presence of entanglement in the wave function. Quantum entanglement occurs when two or several particles participate to a quantum state whose wave function cannot be described as a (properly symmetrized or antisymmetrized) product of the wave functions of the individual particles, *even in absence of any physical interaction among the particles*. In other terms, there is a correlation between the particles even if they do not interact, for instance, for being separated by infinite distances. Broadly speaking, we have quantum entanglement if two subsystems that compose a system "interact" in such a way that the quantum state of each subsystem cannot be described independently: a quantum state may be given only for the system as a whole, *even in the case of two particles separated by a very large (in principle, also infinite) distance*. In the language of quantum chemistry, the entanglement is often (although not always) associated to the presence of non-dynamical correlation. In this case, several Slater determinants are needed for a correct description of the system, even if their parts are not related by a physical interaction. As an example, let us consider a hydrogen dimer at very large inter-nuclear distance. We have *spin* entanglement in the case of the lowest "neutral" symmetric singlet, $1^1\Sigma_g^+$, and the $S_z = 0$ component of the first antisymmetric triplet, $1^3\Sigma_u^+$: the presence of an electron having a given spin on one center implies the presence of an electron having opposite spin on the other center, and vice versa. Analogously, we have *charge* entanglement in the case of "ionic states," like the lowest antisymmetric singlet, $1^1\Sigma_u^+$: the presence of two electrons on one center implies the absence of electrons on the other center, and vice versa. Notice that the two other components of the triplet, on the other

hand, admit a single-determinant localized description, and no entanglement is present in this case. As illustrated in this work, the presence of charge entanglement in the H_2 molecule leads to a SS-TPS tensor that quadratically grows with the distance at large distance. In a similar way, spin entanglement leads to an analogous behavior of the partitioned SP-TPS tensor.

The notion of entanglement is a subtle one, and a discussion of this concept, even in the simple case of the hydrogen dimer, is certainly outside the purpose of the present work. It is interesting to notice, however, that the entanglement can be generalized to the limit case of a *single particle*. A very interesting discussion of this situation can be found, for instance, in Ref. 49. In this work it is argued, in particular, that a state of the form "$|0\rangle |1\rangle + |1\rangle |0\rangle$ is entangled." This is in agreement with the behavior of the TPS for the g and u states of the H_2^+ ion, as illustrated in Table II. Let us now consider in detail the two low-lying doublet ions, $|^2\Sigma_g^+\rangle$ and $|^2\Sigma_u^+\rangle$. They have an identical expression for the asymptotic spread, namely,

$$\lim_{R\to\infty} \Lambda^\parallel(^2\Sigma_g^+) = \lim_{R\to\infty} \Lambda^\parallel(^2\Sigma_u^+) = \frac{1}{Z^2} + \frac{R^2}{4}. \quad (47)$$

In this case, the single electron is equally distributed on both nuclei so we have charge and spin entanglement.

The ground-state symmetric singlet bears a single electron on each atom, and so does the triplet. For the states $^1\Sigma_g^+$, we have that

$$\lim_{R\to\infty} \theta(R) = \pm\frac{\pi}{4}, \quad (48)$$

where the $-$ sign holds for the ground and $+$ for the excited $^1\Sigma_g^+$ state, respectively. Therefore we have

$$\lim_{R\to\infty} \Lambda^\parallel(1^1\Sigma_g^+) = \lim_{R\to\infty} \Lambda^\parallel(^3\Sigma_u^+) = \frac{2}{Z^2}. \quad (49)$$

In other words, the long-distance value of both states converges toward twice the value of a single atom. The antisymmetric singlet, on the other hand, has either zero or two electrons

on each atom. For this reason, beside the atomic contribution (the same as in the previous cases), there is a delocalization contribution that diverges as R^2,

$$\lim_{R\to\infty} \Lambda^{\|}(^1\Sigma_u^+) = \frac{2}{Z^2} + R^2. \tag{50}$$

The same asymptotic behavior is shown by the excited singlet $2^1\Sigma_g^+$,

$$\lim_{R\to\infty} \Lambda^{\|}(2^1\Sigma_g^+) = \frac{2}{Z^2} + R^2. \tag{51}$$

Let us consider now the $\alpha\alpha$ and $\beta\beta$ terms (the $\alpha\beta + \beta\alpha$ term being obtained by simple difference between the total contribution and the $\alpha\alpha + \beta\beta$ one). In the ground-state singlet, an α electron is either on atom A or atom B, being $1/2$ the average of α electrons on each atom. Therefore, $\Lambda^{\|}_{\alpha\alpha}$ will bear the contribution of a single hydrogen atom, plus a delocalization term given by $R^2/2$. The same will happen for $\Lambda^{\|}_{\beta\beta}$. This explains why the long-range behavior of $\alpha\alpha + \beta\beta$ is exactly the same as for the $S_z = 0$ component of the triplet. In the case of the $\bar{S}_z = \pm 1$, on the other hand, there is no fluctuation, and the $\alpha\alpha$ (respectively, $\beta\beta$) components of $^{3(1)}\Sigma_u^+$ (respectively, $^{3(-1)}\Sigma_u^+$) are given by the total contribution.

We consider now the case of a single Slater determinant of atomic spin-orbitals, chosen between the two determinants that give rise to the singlet ground state and the triplet. Let us take, for instance, the determinant $|A\bar{B}\rangle$. First of all, we remind that

$$\langle A|\hat{R}_\alpha|A\rangle = -\frac{R}{2}, \text{ and } \langle \bar{B}|\hat{R}_\beta|\bar{B}\rangle = \frac{R}{2}. \tag{52}$$

At long inter-atomic distance, when the atomic overlap can be neglected, the determinant $|A\bar{B}\rangle$ is normalized. We have

$$\langle A\bar{B}|\hat{R}_\alpha|A\bar{B}\rangle = \frac{R}{2},$$
$$\langle A\bar{B}|\hat{R}_\beta|A\bar{B}\rangle = -\frac{R}{2},$$
$$\langle A\bar{B}|\hat{R}_\alpha\hat{R}_\alpha|A\bar{B}\rangle = \langle A\bar{B}|\hat{R}_\beta\hat{R}_\beta|A\bar{B}\rangle = \frac{1}{Z^2} + \frac{R^2}{4},$$
$$\langle A\bar{B}|\hat{R}_\alpha\hat{R}_\beta|A\bar{B}\rangle = \langle A\bar{B}|\hat{R}_\beta\hat{R}_\alpha|A\bar{B}\rangle = -\frac{R^2}{4}.$$

Therefore, for the spin-partitioned TPS tensor, we obtain

$$\lim_{R\to\infty} \Lambda^{\|}_{\alpha\alpha}(A\bar{B}) = \lim_{R\to\infty} \Lambda^{\|}_{\beta\beta}(A\bar{B}) = \frac{1}{Z^2} \tag{53}$$

and

$$\lim_{R\to\infty} \Lambda^{\|}_{\alpha\beta}(A\bar{B}) = \lim_{R\to\infty} \Lambda^{\|}_{\beta\alpha}(A\bar{B}) = 0. \tag{54}$$

Notice that the same result can be obtained, in a more straightforward way, simply by evaluating the mean values in the coordinate system having the origin in $-\frac{R}{2}$ (for $\Lambda^{\|}_{\alpha\alpha}$) and $\frac{R}{2}$ (for $\Lambda^{\|}_{\beta\beta}$).

All these results are summarized in Table II, where the hydrogen value for the nuclear charge has been assumed ($Z = 1$). As a general conclusion, we see that, each time that the system has a large-distance asymptotic wave function that is composed of two different ionic Slater determinants, the spread tensor contains quadratically growing terms. This is the case of the ionic $^1\Sigma_u^+$ state which becomes $|A\bar{A}\rangle - |B\bar{B}\rangle$ or

the ionic excited singlet $2^1\Sigma_g^+$ which becomes $|A\bar{A}\rangle + |B\bar{B}\rangle$. In other words, if there is a *charge fluctuation* in the wave function, then both the spin-summed and spin-partitioned spreads have a quadratic growth. In presence of a *spin fluctuation* only (with non-fluctuating total charge, like in the case of the $1^1\Sigma_g^+$ ground state), the quadratically growing terms are $\Lambda_{\alpha\alpha+\beta\beta}$ and $\Lambda_{\alpha\beta+\beta\alpha}$, but not their sum Λ. It is interesting to notice that, in each one of these cases, this behavior is due to the interaction terms between the determinants contributing to the wave function.

IV. FULL-CI RESULTS

In this section, the results obtained at FCI level on the hydrogen dimer treated through a high-quality basis set, as well as on hydrogen chains in which we used a set of 1s STO-12G is discussed. With this symbol, we mean a 1s Slater orbital expanded as a contraction of 12 gaussian orbitals, as it is specified later.

A. Computational details

The full CI calculations presented in this work were performed using the NEPTUNUS code.[50–53] This is a FCI code for the calculation of the wave function and the associated spreads, and it uses the Hamiltonian and position integrals produced by the DALTON chain.[54] The interface between the two codes is done through the Q5Cost formalism.[55–58]

We performed FCI calculations on open linear chains described by a Hubbard Hamiltonian[29] (HubL_n), for an even number n of centers going from 2 to 14. In its simplest form, the Hubbard Hamiltonian is given by

$$H = -t \sum_{\langle i,j \rangle} \sum_{\sigma=\alpha,\beta} c^+_{i,\sigma} c_{j,\sigma} + U \sum_i n_{i,\alpha} n_{i,\beta}, \tag{55}$$

where $c_{i,\sigma}$ ($c^+_{i,\sigma}$) are annihilation (creation) operators, respectively, of an electron with spin projection σ. In this equation, the sum over i runs over the system sites, while $\langle i,j \rangle$ indicates topologically connected sites. The parameter t is the hopping integral between the connected sites i and j, while U is the one-center Coulomb repulsion. Although many properties of this model, like the total energy or the energy gap, admit an analytical expression,[59] the analytical calculation of the spread is not trivial, and we computed the TPS tensors numerically using our FCI code.

We also performed FCI calculations on the H_2 dimer by employing the V6Z valence basis set of Dunning,[60] which is a basis of $(10s,5p,4d,3f,2g,1h)$ gaussian primitives contracted to $(6s,5p,4d,3f,2g,1h)$.

Finally, we treated at FCI level using the minimal STO-12G basis set the H_n ($n = 2,4,6,8,10,12,14,16$) linear chains with equally spaced atoms. This STO-12G expansion was obtained in the following way. We took the 12 gaussian primitives of s type of the basis set of Tunega and Noga[61] and computed the wave function of a H atom to get the expansion coefficients. In this way, a very accurate description of the isolated atom is obtained, with an energy of $-0.499\,998\,632\,164$ hartree instead of the exact value of -0.5 hartree.
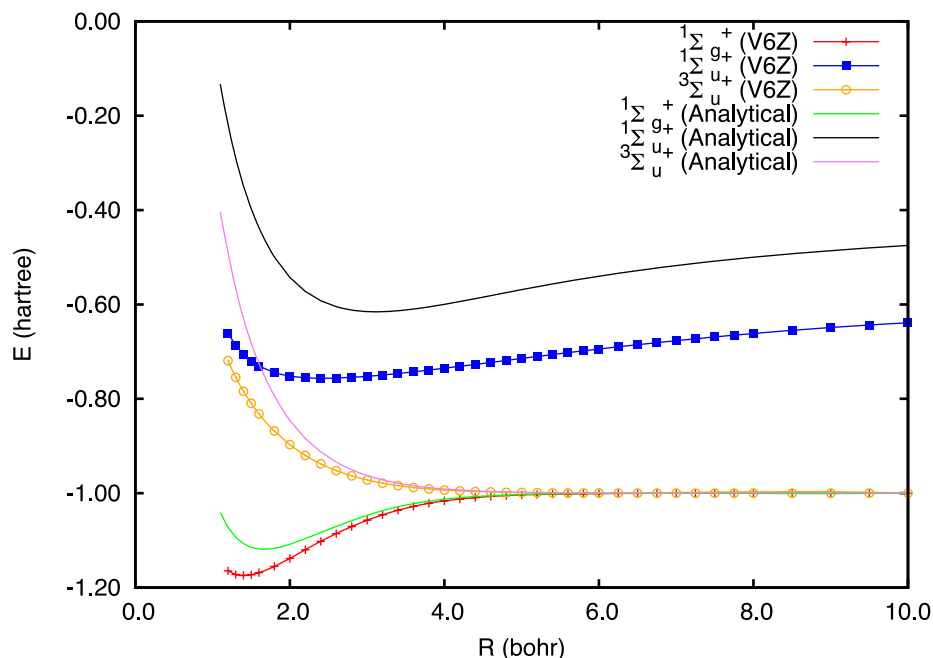
FIG. 1. Total energies for the $^1\Sigma_g^+$, $^1\Sigma_u^+$, and $^3\Sigma_u^+$ low-lying electronic states of the hydrogen molecule computed at FCI level with the V6Z basis set of Dunning, and values calculated analytically.

B. The hydrogen dimer

We discuss now the FCI treatment of the hydrogen dimer obtained by using the large V6Z basis set, that is able to give an accurate description of this system. We concentrate our attention on the lowest states of each one of the three symmetries considered in Sec. III. In fact, the second symmetric singlet state, $2^1\Sigma_g^+$, has a very different behavior with respect to the corresponding state obtained with the STO basis set, since it undergoes a series of avoided crossings, and its nature changes as a function of the distance. In Figure 1, we report the total energies of the three lowest states, $^1\Sigma_g^+$, $^3\Sigma_u^+$, and $^1\Sigma_u^+$ as a function of the inter-nuclear distance.

In Figures 2–5, we compare the analytical STO results (full lines) with the FCI results (dots). Generally speaking, the two results differ for short distances, because of both orbital relaxation and electron correlation. At large distances, on the other hand, the quality of the STO results with respect to the FCI/V6Z ones depends on the nature of the states: the $^1\Sigma_g^+$ and $^3\Sigma_u^+$ states are purely neutral, and the analytical STO description is exact at dissociation. This means that the FCI and the analytical results at large distance are asymptotically identical. The antisymmetrical singlet, on the other hand, is purely ionic at all distance for symmetry reasons. Therefore, the uncorrelated analytical STO description and the high-quality FCI/V6Z do not coincide, even asymptotically. Moreover, the nature of
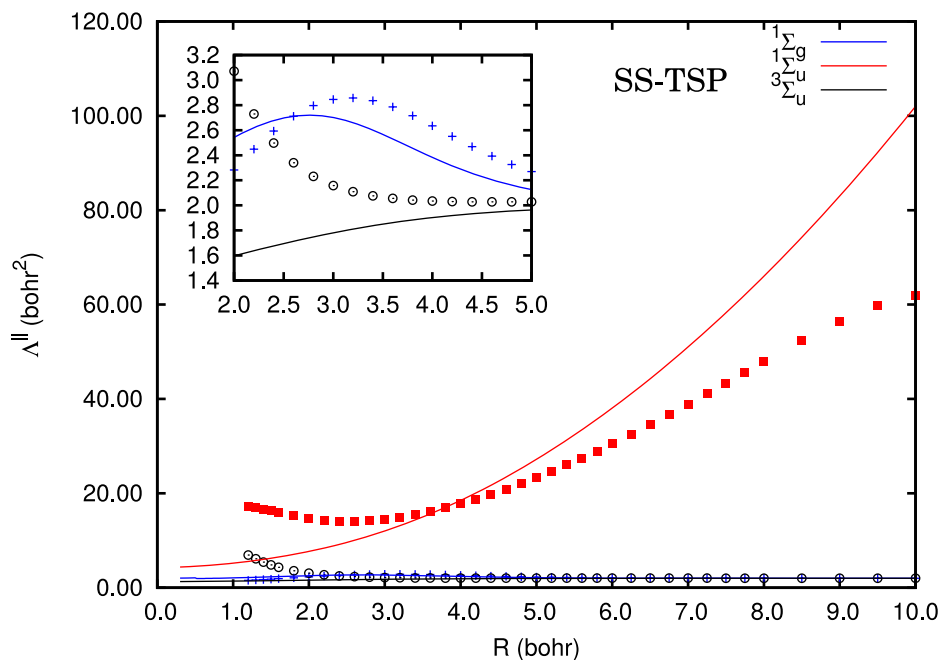

FIG. 2. Longitudinal spin-summed position spread for the $^1\Sigma_g^+$, $^1\Sigma_u^+$, and $^3\Sigma_u^+$ low-lying electronic states of the hydrogen molecule computed at FCI level with the V6Z basis set of Dunning. Full lines represent values calculated analytically.
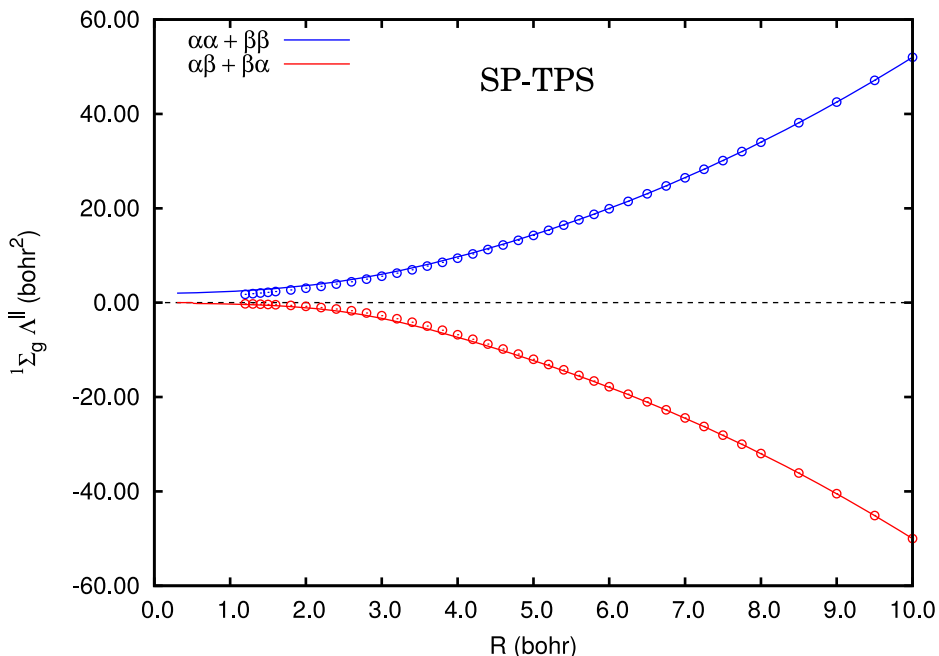
FIG. 3. Longitudinal spin-partitioned position spread for the $^1\Sigma_g^+$ electronic state of the hydrogen molecule computed at FCI level with the V6Z basis set of Dunning. Full lines represent values calculated analytically.

the FCI/V6Z state changes strongly with the distance, because of a series of avoided crossing.

C. Hubbard chains

We performed FCI calculations on open linear chains described by a Hubbard Hamiltonian[29] (HubL_n), for an even number n of centers going from 2 to 14. The values of the TPS tensors are reported in Figures 6 and 7, as a function of the ratio $-t/U$ and for the different values of n. Notice that, at half filling and for $-t/U = 0$, the magnetic manifold becomes completely degenerate, since all the determinants having one electron per site have a total energy exactly equal to zero. The corresponding values of the spread, on the other hand, are in general not degenerate, so only the limit for $-t/U \to 0$ of the

ground-state spread is meaningful. In practice, for numerical reasons, we stopped our investigation at $-t/U = 0.01$, and we did not consider smaller values.

In Figure 6, we show the SS-TPS values. For $-t/U \to 0$, $\Lambda_\parallel$ vanishes regardless the value of n, since at half filling, we have exactly one electron on each center. For large values of the ratio $-t/U$, the $\Lambda_\parallel(n)/n$ converge, in a rather slow way, toward the uncorrelated limit. At $-t/U = \infty$, we get a Hückel chain, and $\Lambda_\parallel(n)/n$ has a linear growth as a function of n (the chain is a metallic system).[15] The behavior of the SP-TPS tensor is illustrated in Figure 7. For small values of $-t/U$, the equal-spin and different-spin components, $\Lambda_{\alpha\alpha+\beta\beta}^\parallel(n)/n$ and $\Lambda_{\alpha\beta+\beta\alpha}^\parallel(n)/n$, respectively, have the same absolute value and opposite sign, in such a way that the spin-summed value vanishes. For large values of $-t/U$, the equal-spin components
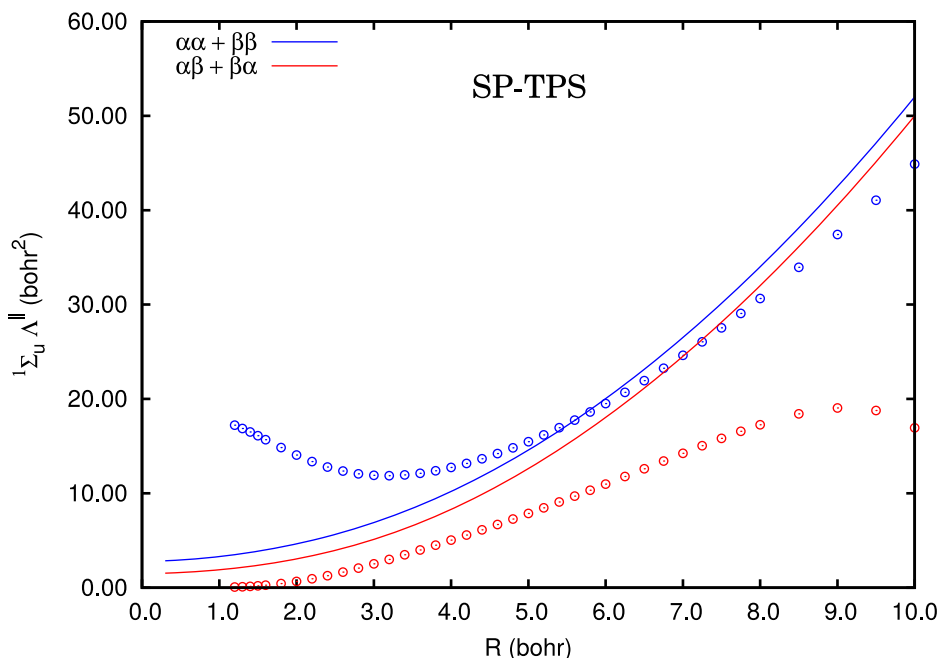

FIG. 4. Longitudinal spin-partitioned position spread for the $^1\Sigma_u^+$ electronic state of the hydrogen molecule computed at FCI level with the V6Z basis set of Dunning. Full lines represent values calculated analytically.
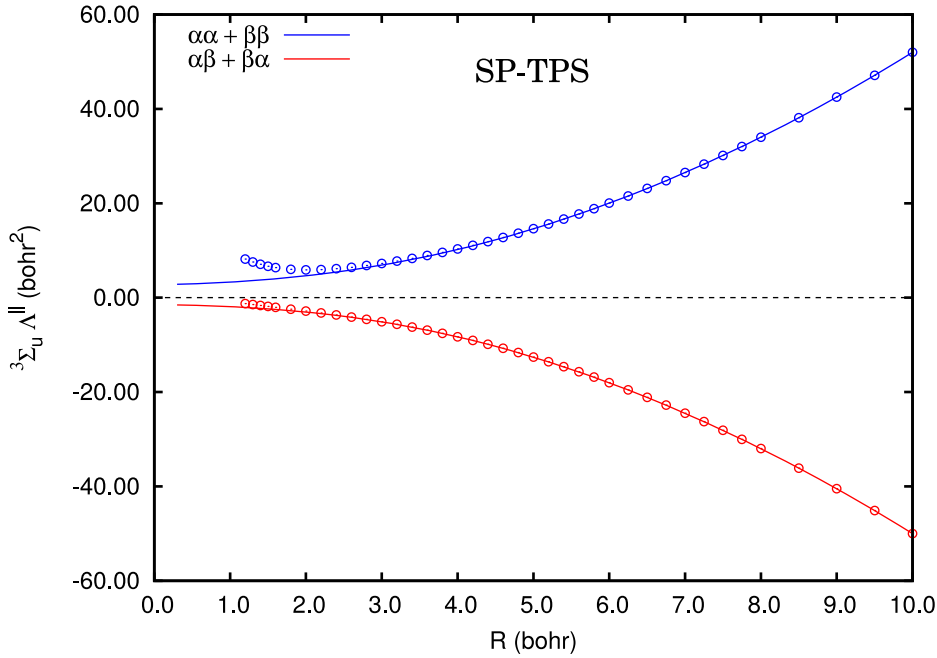
FIG. 5. Longitudinal spin-partitioned position spread for the $^3\Sigma_u^+$ electronic state of the hydrogen molecule computed at FCI level with the V6Z basis set of Dunning. Continuous lines are the analytical results.

quickly saturate to a value that has a linear growth as a function of n, while the different-spin components slowly converge to zero. This explains the slow convergence of the SS-TPS for large values of $-t/U$.

D. Hydrogen chains

The case of non-dimerized linear hydrogen chains (HL_n) is discussed in this section. These chains were studied at FCI level employing the basis set STO-12G. For n greater than two, even by using a minimal basis set, this system admits only numerical solutions. In the case of chains, the comparison of systems having a different number of centers plays a crucial role. For this reason, the TPS values reported in this section are often divided by the number of atoms of the systems.

The behavior for large values of n is particularly relevant, since it gives information on the "metallicity" of the system.[2] Unfortunately, the convergence towards the asymptotic regime as a function of n is rather slow. Since calculations involving large values of n become prohibitively expensive (the largest accessible system is for $n = 18$, at a price of a huge computational effort), extrapolation techniques are needed for such an investigation. In the following parts of this section, the spin-summed and spin-partitioned tensors will be separately discussed.

1. The spin-summed spread

In Figure 8, the FCI energies *per atom* are reported as a function of the inter-atomic distances R, for the HL_n (n = 2, 4, 6, 8, 10, 12, 14, 16). For all the involved chains except the
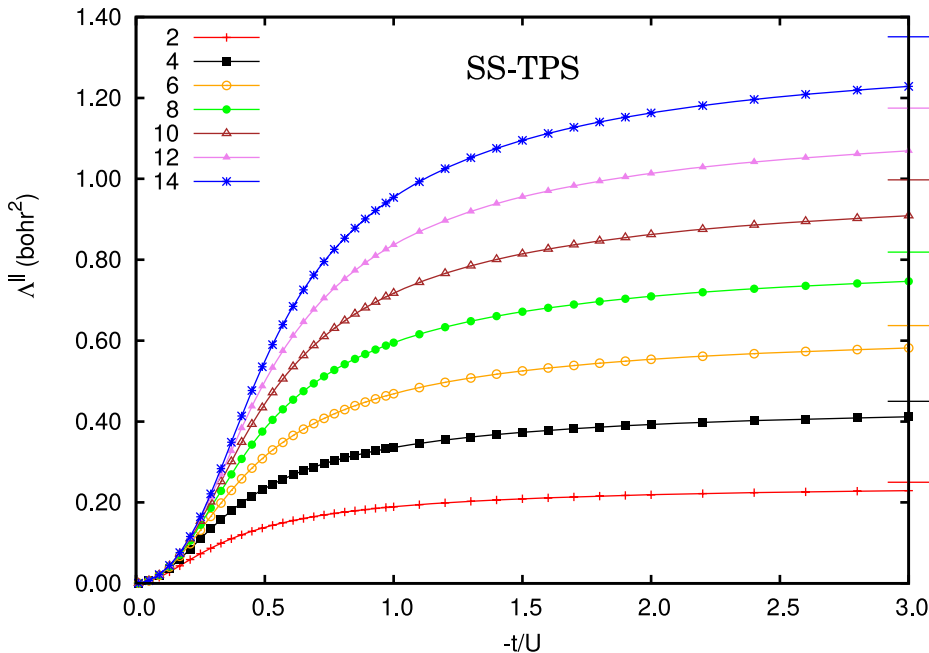

FIG. 6. Total position spread tensor for non-dimerized open Hubbard chains divided by the number of sites. The marks in the right vertical axis represent the uncorrelated limit.
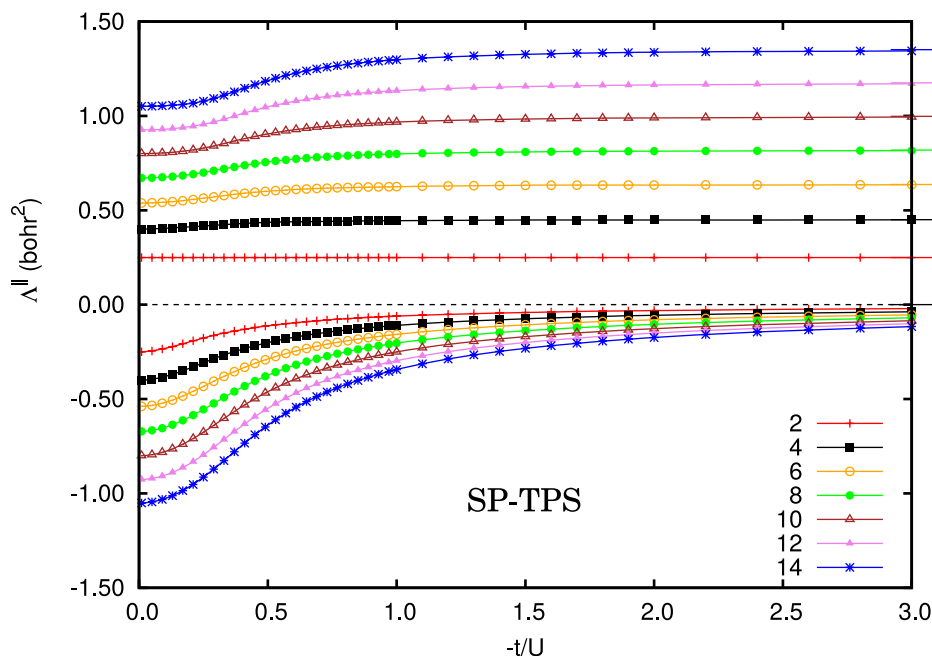
FIG. 7. Spin-partitioned position spread tensor for non-dimerized open Hubbard chains divided by the number of sites. Positive values represent the $\alpha\alpha$ component, and negative values the $\alpha\beta$ component of the tensor. The marks in the right vertical axis represent the uncorrelated limit.

dimer, there is a minimum of the potential energy surfaces (PES) in the region of 2.0 bohrs. It is remarkable to note that the values of *per atom* energies are superposed for inter-atomic distances larger than 2.2 bohrs. However, near the equilibrium distance, H_2 is slightly more stable than the longer chains. These superposed *per atom* energies mean that the border effects are small in these systems. These results are consistent with those calculated for periodic hydrogen chains at variational Monte Carlo (VMC) level by Stella *et al.*[34] However, the curves shown therein are lower than the ones we report because VMC allows for a much better (but approximate) description of correlation effects than FCI. In fact, the basis set employed at VMC level consisted of $3s$ orbitals for the geminal part, and $2s2p$ for the Jastrow part (see Eqs. 1-2 in Ref. 34).

The behavior of the total position spread tensor calculated at the same level of theory is now considered. The TPS is closely related to the metallic vs insulator character of a molecular system. For a set of n non-interacting electrons occupying a region of length L of the space, the spread is expected to be of the order of L^2. This behavior is observed, for instance, in the case of non-interacting particles in a box[16] and Hückel Hamiltonians.[15] In the thermodynamic limit, the spread of the electrons is expected to diverge. In Figure 9, the *per atom* values of the longitudinal component of the TPS ($\Lambda^{\parallel}$) are shown as a function of the inter-atomic distances. As a first observation, for all chains involved, the value of $\Lambda^{\parallel}/n$ for inter-atomic distances that tend to infinity converges to the isolated-atom value (1 bohr^2).
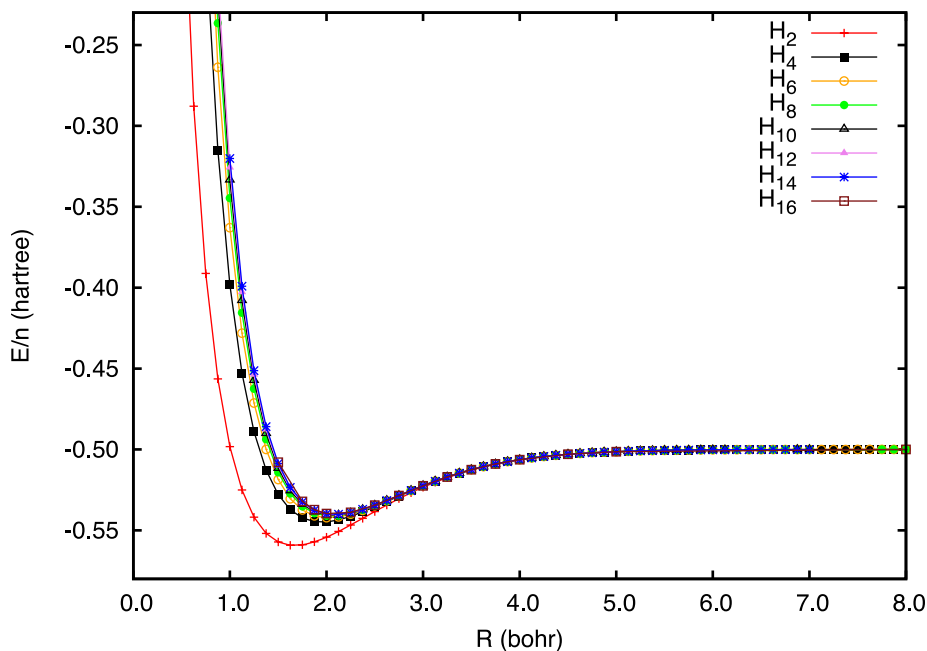

FIG. 8. Potential energy curves of hydrogen chains per atoms calculated at FCI level and employing the minimal basis set STO-12G.
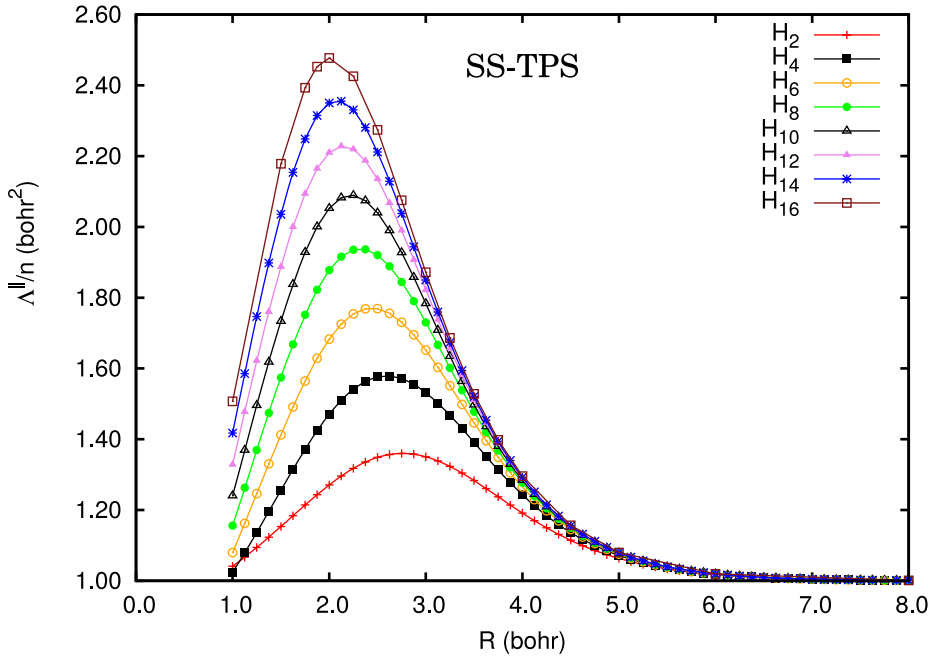
FIG. 9. Total position spread tensor for the different hydrogen chains divided by the number of atoms at FCI level and the minimal basis set STO-12G.

On the contrary, for distances below 1 bohr, nuclei are closer and the nuclear effective charge experienced by the electrons is higher. At the same time, this leads to a spatial contraction and then electrons are more localized. For R values near to the equilibrium distance, the TPS increases and keeps growing until it reaches a marked maximum close to the bond-breaking distance. At such molecular configuration, the systems show a maximum delocalization of the wave function due to a rearrangement of the electrons to occupy one $1s$ atomic orbital at dissociation. It is important to note that the magnitudes of the maxima increase (and get displaced to shorter values of R) with the size of the molecular chains (see Figure 9).

Let us now compare the SS-TPS results with the values of the localization tensor λ_N reported in Ref. 34. In the insulating regime (at large values of R), both $\Lambda^{\parallel}/n$ and λ_N do not depend on the size of the molecules and the curves are superposed. Then, for values below 5 bohrs, $\Lambda^{\parallel}/n$ and λ_N start to show a dependency on the number of atoms in the system. This indicates a Mott transition,[38] from an antiferromagnetic insulator ($S_z = 0$ for our hydrogen chains calculations) to a metal in the region of R between 3.5 and 2.0 bohrs.

In order to investigate the behavior of the specific parallel spread $\Lambda^{\parallel}(n)/n$ in the different distance regions, it is convenient to extrapolate the spread values, for a fixed inter-nuclear distance, as a function of the number of atoms. By assuming, for large n and at a fixed R value, a linear functional form of the type

$$\Lambda^{\parallel}(R,n)/n = \Lambda_0^{\parallel}(R) + \Lambda_1^{\parallel}(R)n \tag{56}$$

(i.e., by truncating a power expansion in n to the first two terms), the values of $\Lambda_0^{\parallel}(R)$ and $\Lambda_1^{\parallel}(R)$ can be graphically obtained. Indeed, one can plot the quantity $\Lambda^{\parallel}(R,n)/n^2$ as a function of $1/n$ and extrapolate the curve for $1/n \to 0$. See Figures SM1 and SM3 in the supplementary material,[48] where

$\Lambda_{\parallel}(R,n)/n^2$ as a function of $1/n$ for $R = 2$ and $R = 6$ bohrs are reported. By performing the extrapolation for $1/n \to 0$, we obtain for $\Lambda_0^{\parallel}(R)$ and $\Lambda_1^{\parallel}(R)$ the values $\Lambda_0^{\parallel}(2) = 1.088\,66$ and $\Lambda_1^{\parallel}(2) = 0.259\,27$ for $R = 2.0$ bohrs, and $\Lambda_0^{\parallel}(6) = 1.016\,53$ and $\Lambda_1^{\parallel}(6) = 2.925\,92 \times 10^{-4}$ for $R = 6.0$ bohrs. This means that the spread is practically constant for $R = 6.0$ bohrs, while it has a linear growth for $R = 2.0$ bohrs. These results can be interpreted as a metallic behavior at short inter-atomic separation and an insulator at large separation.

2. The spin-partitioned spread

The spin-partitioned parallel spreads are now discussed. In Figure 10, the spin-partitioned longitudinal spreads, $\Lambda_{\alpha\alpha+\beta\beta}^{\parallel}$ and $\Lambda_{\alpha\beta+\beta\alpha}^{\parallel}$, are reported. It appears that they have similar absolute values but opposite signs, in such a way that the spin-summed spread is only a very small fraction of the spin-partitioned terms. Moreover, the two terms quickly diverge for increasing values of both n and R.

The behavior of the spin-partitioned tensor for large values of n and R can also be graphically investigated. For a fixed value of n, the curves of $\Lambda_{\alpha\alpha+\beta\beta}(n,R)/R^2$ become constant for large values of R, indicating a quadratic dependence on R. Again, the dependence on n is more difficult to study, since calculations for large n values are impossible. In order to investigate this aspect, the curves corresponding to $\Lambda_{\alpha\alpha+\beta\beta}(n,R)/(n^2R^2)$ are plotted, as a function of R, for different values of n. This is illustrated in Figure SM2 (in the supplementary material[48]) where the quadratic dependence from R for large R values clearly appears. Moreover, it can be seen that the different curves tend to a common limit for large values of n. In fact, if the same quantity is plotted, for a *fixed* large value of R, as a function of $1/n$, an extrapolated value for $n \to \infty$ can be obtained. (See the plot for $R = 6$ bohrs in Figure SM4, in the supplementary material.[48]) These results
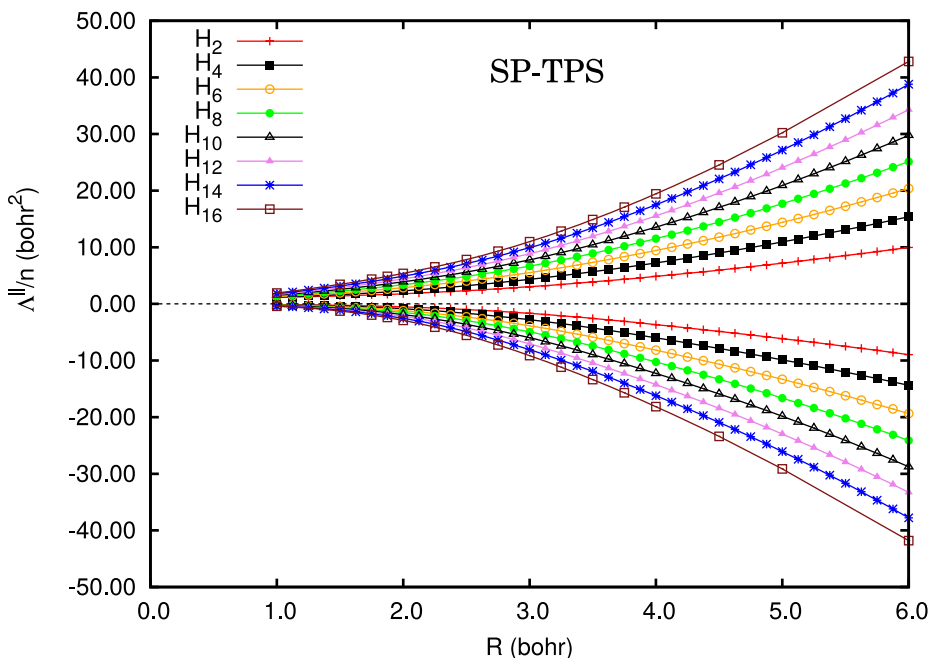
FIG. 10. Spin-partitioned position spread tensor for the different hydrogen chains divided by the number of atoms at FCI level and the minimal basis set STO-12G. Positive values represent the $\alpha\alpha + \beta\beta$ contribution, and negative values the $\alpha\beta + \beta\alpha$ contribution.

imply that the asymptotic values of the equal-spin term can be expressed, for large values of n and R, as a function of the form

$$\Lambda_{\alpha\alpha+\beta\beta}(N,R)/n = C_{\alpha\alpha+\beta\beta}nR^2, \tag{57}$$

where $C_{\alpha\alpha+\beta\beta}$ is a dimensionless constant.

It is possible to extrapolate the values of $\Lambda_{\alpha\alpha+\beta\beta}(n,R)$ for large values of n, as it was done for the total spread in Sec. IV D 1. We assumed a two-term linear expansion

$$\Lambda^{\|}_{\alpha\alpha+\beta\beta}(R,n)/n = \Lambda^{\|}_{\alpha\alpha+\beta\beta,0}(R) + n\Lambda^{\|}_{\alpha\alpha+\beta\beta,1}(R). \tag{58}$$

For $R = 6.0$ bohrs, the extrapolated values of $\Lambda^{\|}_{\alpha\alpha+\beta\beta,0}(6) = 2.445\,87$ and $\Lambda^{\|}_{\alpha\alpha+\beta\beta,1}(6) = 5.220\,63$ are obtained, showing a divergent behavior of $\Lambda^{\|}_{\alpha\alpha+\beta\beta}(R,n)/n$ as a function of n.

For a fixed number of centers, $\Lambda_{\alpha\alpha+\beta\beta}$ grows as the square of R, as shown in Figure SM2 (in the supplementary material[48]). This implies that the equal-spin TPS grows as the square of the chain total length. Notice that the different-spin term, $\Lambda^{\|}_{\alpha\beta+\beta\alpha}(R,n)/n$, has asymptotically the same form, but opposite sign. It is interesting to compare these results with the behavior of the uncorrelated electrons of a linear Hückel chain. Indeed, for large inter-nuclear distances, the $\alpha\alpha + \beta\beta$ longitudinal spread has the same behavior of the total longitudinal spread of the Hückel chains.[15] This fact indicates a large spin mobility in non-dimerized chains for large values of R. As discussed in Subsection IV D 1, this is the opposite to what happens for the charge mobility.

V. CONCLUSIONS

In the present work, the partition of the total-position spread tensor according to its spin components has been presented. In particular, the equal-spin and different-spin components have been defined, and their behavior has been inves-

tigated in the case of some simple systems. As for the spin-summed tensor, both spin components are invariant with respect to translations, and additive in the case of factorizable wave functions of non-interacting subsystems. Moreover, their trace is invariant with respect to rotations. For these reasons, these tensors are truly invariant quantities that can be associated to a physical system, like the energy and the polarizability.

The formalism has been illustrated through applications to different hydrogen systems:

1. The hydrogen dimer described by a STO orbital. This model system admits a fully analytical treatment.
2. The same H_2 dimer described at full-CI level by means of a rather large V6Z basis set, that is able to give a realistic description of this molecule.
3. Equally spaced hydrogen linear chains, H_n, treated at full-CI level and by using a single STO-12G contracted gaussian orbital for each hydrogen atom.

The results for the H_2 dimer show a divergent behavior of the two spin-partitioned longitudinal components of the spread tensor, $\Lambda^{\|}_{\alpha\alpha+\beta\beta}$ and $\Lambda^{\|}_{\alpha\beta+\beta\alpha}$, at large inter-nuclear distances in some cases. This divergence is related to the presence of entanglement in the long-range wave function. In particular, the divergence of the spin-summed TPS tensor $\Lambda^{\|}$ is associated to *charge* entanglement, and this is the case for the $^1\Sigma_u^+$ excited state. The divergence of the spin-partitioned components $\Lambda^{\|}_{\alpha\alpha+\beta\beta}$ and $\Lambda^{\|}_{\alpha\beta+\beta\alpha}$, on the other hand, is associated to *spin* entanglement (in the $^1\Sigma_g^+$ ground state, and the $S_z = 0$ component of the $^3\Sigma_u^+$ triplet). No divergence at all is shown by the other spin components of the triplet, for which no entanglement is present in the wave function.

A similar behavior is found in the case of the H_n chains, for which both $\Lambda^{\|}_{\alpha\alpha+\beta\beta}$ and $\Lambda^{\|}_{\alpha\beta+\beta\alpha}$ diverge at large inter-nuclear distance. Moreover, also the *per-electron* value of these tensors diverge as a function of the electron number. This

is a behavior very much similar to that of the spin-summed tensor in the case of conductors and is related to the presence of highly correlated magnetic wave functions for these chains at large distances and number of atoms. Work is in progress in our group on other types of magnetic models, like Heisenberg Hamiltonians (having both ferromagnetic or antiferromagnetic couplings) or dimerized hydrogen chains, in order to elucidate the relation between the wave function magnetic character of these systems and the behavior of the SP-TPS tensors.

The TPS tensor gives information on the mobility of the electrons in molecules or extended systems. For this reason, it had been shown to be a powerful tool to describe the mobility of the electrons in charge-transfer systems, and in the theory of conductivity for metallic systems in particular. In the same way, the spin-partitioned TPS tensors we introduced in this work provide information on the mobility of the *spins*. This is of particular interest in all those cases where this mobility is not associated to charge-transfer processes, and for which the spin-summed TPS tensor is not capable to provide the relevant information. For these reasons, we believe that the spin-partitioned TPS tensor will be a powerful tool to investigate the behavior of the electrons in highly correlated systems, and in particular the propagation of magnetic modes in magnetic structures.

APPENDIX: MATRIX ELEMENTS OF THE POSITION OPERATOR IN THE AO BASIS, AND SIZE ADDITIVITY OF CUMULANTS

1. Matrix elements over 1s STO

The overlap between the two 1s atomic orbitals, s_{AB}, is given by

$$s_{AB} \equiv \langle 1s_A | 1s_B \rangle = e^{-ZR}\left(1 + ZR + \frac{Z^2 R^2}{3}\right). \quad (A1)$$

For the matrix elements of $\hat{z}$ on the AO basis, we have

$$\langle A_\sigma | \hat{z}_\sigma | A_\sigma \rangle = -\frac{R}{2} \quad (A2)$$

and

$$\langle B_\sigma | \hat{z}_\sigma | B_\sigma \rangle = \frac{R}{2} \quad (A3)$$

while

$$\langle A_\sigma | \hat{z}_\sigma | B_\sigma \rangle = \langle B_\sigma | \hat{z}_\sigma | A_\sigma \rangle = 0 \quad (A4)$$

because $1s_A(\mathbf{r})1s_B(\mathbf{r})$ is an even function of z.

For the matrix elements of $\hat{x}$ on the AO basis, we have

$$\langle A_\sigma | \hat{x}_\sigma | A_\sigma \rangle = \langle B_\sigma | \hat{x}_\sigma | B_\sigma \rangle = \langle A_\sigma | \hat{x}_\sigma | B_\sigma \rangle = 0. \quad (A5)$$

For the matrix elements of the z^2 operator, on the other hand, we have

$$\langle A_\sigma | \hat{z}_\sigma^2 | A_\sigma \rangle = \langle B_\sigma | \hat{z}_\sigma^2 | B_\sigma \rangle = \frac{R^2}{4} + \frac{1}{Z^2} \quad (A6)$$

while

$$\langle A_\sigma | z_\sigma^2 | B_\sigma \rangle = \langle B_\sigma | z_\sigma^2 | A_\sigma \rangle \equiv z_{AB}^2, \quad (A7)$$

where the integrals in Eq. (A7) have the expression (see Ref. 62)

$$z_{AB}^2 = e^{-ZR}\left(\frac{1}{Z^2} + \frac{R}{Z} + \frac{9R^2}{20} + \frac{7R^3 Z}{60} + \frac{R^4 Z^2}{60}\right). \quad (A8)$$

For the matrix elements of the x^2 operator, on the other hand, we have

$$\langle A_\sigma | \hat{x}_\sigma^2 | A_\sigma \rangle = \langle B_\sigma | \hat{x}_\sigma^2 | B_\sigma \rangle = \frac{1}{Z^2} \quad (A9)$$

while

$$\langle A_\sigma | x_\sigma^2 | B_\sigma \rangle = \langle B_\sigma | x_\sigma^2 | A_\sigma \rangle \equiv x_{AB}^2, \quad (A10)$$

where

$$x_{AB}^2 = e^{-ZR}\left(\frac{1}{Z^2} + \frac{R}{Z} + \frac{2R^2}{5} + \frac{R^3 Z}{15}\right). \quad (A11)$$

2. Size additivity

It is well known that the cumulant of a composite system is equal to the sum of the cumulants of its parts provided the latter are independent.[44] This might be the case of a molecule dissociating in two separate fragments. Here, we briefly re-derive this property having in mind the TPS tensor. We assume that the wave function of the composite system ψ_{AB} is the anti-symmetrized product of ψ_A and ψ_B. The wave function of each fragment F will be expressed in the form of a CI expansion,

$$\psi_F = \Sigma_i f_i \hat{\pi}_i^\dagger | 0 \rangle = \hat{O}_F^\dagger | 0 \rangle, \quad F = A, B, \quad (A12)$$

where f_i are the CI coefficients, $\hat{\pi}_i^\dagger$ is a product of n_F creation operators, and $|0\rangle$ is the vacuum state. We consider now the case when the fragments A, B are at infinite distance so the orbitals of A and those of B are completely disjoint, in such a way that the following equations hold:

$$\langle \psi_{AB} | \psi_{AB} \rangle = \langle 0 | \hat{O}_A \hat{O}_A^\dagger | 0 \rangle = \langle 0 | \hat{O}_B \hat{O}_B^\dagger | 0 \rangle = 1,$$
$$|\psi_{AB}\rangle = \hat{O}_A^\dagger \hat{O}_B^\dagger | 0 \rangle = (-)^{n_A n_B} \hat{O}_B^\dagger \hat{O}_A^\dagger | 0 \rangle. \quad (A13)$$

Equation (A13) is a trivial consequence of the anti-commutation relations and one also has the following:

$$\hat{O}_A^\dagger \hat{O}_B^\dagger = (-)^{n_A n_B} \hat{O}_B^\dagger \hat{O}_A^\dagger,$$
$$\hat{O}_A^\dagger \hat{O}_B = (-)^{n_A n_B} \hat{O}_B \hat{O}_A^\dagger,$$
$$\hat{O}_A \hat{O}_B^\dagger = (-)^{n_A n_B} \hat{O}_B^\dagger \hat{O}_A,$$
$$\hat{O}_A, \hat{O}_B = (-)^{n_A n_B} \hat{O}_B, \hat{O}_A. \tag{A14}$$

We also remind the following equations:

$$\hat{O}_A \hat{O}_A^\dagger |0\rangle = \hat{O}_B \hat{O}_B^\dagger |0\rangle = |0\rangle, \tag{A15}$$

$$\hat{O}_F \hat{\Omega} \hat{O}_F^\dagger |0\rangle = |0\rangle \langle 0|\hat{O}_F \hat{\Omega}\hat{O}_F^\dagger|0\rangle, \; F = A, B. \tag{A16}$$

Last Eq. (A16), where $\hat{\Omega}$ is any number-conserving operator, is trivially due to the zero-electron space being 1-dimensional. Let us now consider a generic element of the TPS tensor

$$\Lambda_{pq} = \langle \psi_{AB}|\hat{P}\hat{Q}|\psi_{AB}\rangle - \langle \psi_{AB}|\hat{P}|\psi_{AB}\rangle \langle \psi_{AB}|\hat{Q}|\psi_{AB}\rangle, \tag{A17}$$

where $\hat{P}$, $\hat{Q}$ are two components (possibly equal) of the total position operator. Suppose now that $\hat{P} = \hat{P}_A + \hat{P}_B$ with

$$[\hat{P}_A, \hat{P}_B] = [\hat{P}_A, \hat{O}_B] = [\hat{P}_B, \hat{O}_A] = \ldots = 0 \tag{A18}$$

and similarly for $\hat{Q}$. One has

$$\langle \psi_{AB}|\hat{P}\hat{Q}|\psi_{AB}\rangle = \langle 0|\hat{O}_B \hat{O}_A \hat{P}_A \hat{Q}_A \hat{O}_A^\dagger \hat{O}_B^\dagger|0\rangle$$
$$+ \langle 0|\hat{O}_B \hat{O}_A \hat{P}_A \hat{Q}_B \hat{O}_A^\dagger \hat{O}_B^\dagger|0\rangle$$
$$+ \langle 0|\hat{O}_B \hat{O}_A \hat{P}_B \hat{Q}_A \hat{O}_A^\dagger \hat{O}_B^\dagger|0\rangle$$
$$+ \langle 0|\hat{O}_B \hat{O}_A \hat{P}_B \hat{Q}_B \hat{O}_A^\dagger \hat{O}_B^\dagger|0\rangle. \tag{A19}$$

Because of Eqs. (A14) and (A16), one can rearrange as follows:

$$\langle \psi_{AB}|\hat{P}\hat{Q}|\psi_{AB}\rangle = \langle 0|\hat{O}_A \hat{P}_A \hat{Q}_A \hat{O}_A^\dagger \hat{O}_B \hat{O}_B^\dagger|0\rangle$$
$$+ \langle 0|\hat{O}_A \hat{P}_A \hat{O}_A^\dagger|0\rangle \langle 0|\hat{O}_B \hat{Q}_B \hat{O}_B^\dagger|0\rangle$$
$$+ \langle 0|\hat{O}_B \hat{P}_B \hat{O}_B^\dagger|0\rangle \langle 0|\hat{O}_A \hat{Q}_A \hat{O}_A^\dagger|0\rangle$$
$$+ \langle 0|\hat{O}_A \hat{O}_A^\dagger \hat{O}_B \hat{P}_B \hat{Q}_B \hat{O}_B^\dagger|0\rangle,$$
$$\langle \psi_{AB}|\hat{P}\hat{Q}|\psi_{AB}\rangle = \langle \psi_A \hat{P}_A \hat{Q}_A \psi_A \rangle \qquad \tag{A20}$$
$$+ \langle \psi_A \hat{P}_A \psi_A\rangle\langle \psi_B \hat{Q}_B \psi_B\rangle$$
$$+ \langle \psi_B \hat{P}_B \psi_B\rangle\langle \psi_A \hat{Q}_A \psi_A\rangle$$
$$+ \langle \psi_B \hat{P}_B \hat{Q}_B \psi_B\rangle.$$

Similarly one also finds

$$\langle \psi_{AB}|\hat{P}|\psi_{AB}\rangle = \langle \psi_A \hat{P}_A \psi_A\rangle + \langle \psi_B \hat{P}_B \psi_B\rangle,$$
$$\langle \psi_{AB}|\hat{Q}|\psi_{AB}\rangle = \langle \psi_A \hat{Q}_A \psi_A\rangle + \langle \psi_B \hat{Q}_B \psi_B\rangle. \tag{A21}$$

From Eqs. (A20) and (A21), one easily finds the result

$$\Lambda_{pq} = \langle \psi_A|\hat{P}_A \hat{Q}_A|\psi_A\rangle - \langle \psi_A|\hat{P}_A|\psi_A\rangle \langle \psi_A|\hat{Q}_A|\psi_A\rangle$$
$$+ \langle \psi_B|\hat{P}_B \hat{Q}_B|\psi_B\rangle - \langle \psi_B|\hat{P}_B|\psi_B\rangle \langle \psi_B|\hat{Q}_B|\psi_B\rangle. \tag{A22}$$

This result also holds for the spin-partitioned operators $\mathbf{R}_{\alpha\alpha}$ and $\mathbf{R}_{\beta\beta}$ because they fulfill same commutation relation (A18) as the spin summed operators plus the following one: $[\mathbf{R}_{\alpha\alpha}, \mathbf{R}_{\beta\beta}] = 0$. Last, from Eq. (16), one finds that Eq. (A22) holds for $\Lambda_{\alpha\beta+\beta\alpha}$ which is not a cumulant.

[1] W. Kohn, Phys. Rev. **133**, A171 (1964).
[2] R. Resta and S. Sorella, Phys. Rev. Lett. **82**, 370 (1999).
[3] C. Sgiarovello, M. Peressi, and R. Resta, Phys. Rev. B **64**, 115202 (2001).
[4] R. Resta, J. Phys.: Condens. Matter **14**, R625 (2002).
[5] R. Resta, Phys. Rev. Lett. **95**, 196805 (2005).
[6] R. Resta, Eur. Phys. J. B **79**, 121 (2011).
[7] I. Souza, T. Wilkens, and R. Martin, Phys. Rev. B **62**, 1666 (2000).
[8] R. Resta, Phys. Rev. Lett. **96**, 137601 (2006).
[9] R. Resta, J. Chem. Phys. **124**, 104104 (2006).
[10] O. Brea, M. El Khatib, C. Angeli, G. L. Bendazzoli, S. Evangelisti, and T. Leininger, J. Chem. Theory Comput. **9**, 5286 (2013).
[11] V. Vetere, A. Monari, A. Scemama, G. L. Bendazzoli, and S. Evangelisti, J. Chem. Phys. **130**, 024301 (2009).
[12] G. L. Bendazzoli, S. Evangelisti, and A. Monari, Int. J. Quantum Chem. **111**, 3416 (2011).
[13] S. Evangelisti, G. L. Bendazzoli, and A. Monari, Theor. Chem. Acc. **126**, 257 (2010).
[14] G. L. Bendazzoli, M. El Khatib, S. Evangelisti, and T. Leininger, J. Comput. Chem. **35**, 802 (2014).
[15] A. Monari, G. L. Bendazzoli, and S. Evangelisti, J. Chem. Phys. **129**, 134104 (2008).
[16] G. L. Bendazzoli, S. Evangelisti, and A. Monari, Int. J. Quantum Chem. **112**, 653 (2012).
[17] J. G. Ángyán, Int. J. Quantum Chem. **109**, 2340 (2009).
[18] J. G. Ángyán, Curr. Org. Chem. **15**, 3609 (2011).
[19] G. L. Bendazzoli, S. Evangelisti, A. Monari, B. Paulus, and V. Vetere, J. Phys.: Conf. Ser. **117**, 012005 (2008).
[20] V. Vetere, A. Monari, G. L. Bendazzoli, S. Evangelisti, and B. Paulus, J. Chem. Phys. **128**, 024701 (2008).
[21] G. L. Bendazzoli, S. Evangelisti, A. Monari, and R. Resta, J. Chem. Phys. **133**, 064703 (2010).
[22] E. Giner, G. L. Bendazzoli, S. Evangelisti, and A. Monari, J. Chem. Phys. **138**, 074315 (2013).
[23] M. El Khatib, T. Leininger, G. L. Bendazzoli, and S. Evangelisti, Chem. Phys. Lett. **591**, 58 (2014).
[24] V. Magnasco, A. Rapallo, and M. Casanova, Int. J. Quantum Chem. **73**, 333 (1999).
[25] V. Magnasco and A. Rapallo, Int. J. Quantum Chem. **79**, 91 (2000).
[26] R. Horodecki, M. Horodecki, and K. Horodecki, Rev. Mod. Phys. **81**, 865 (2009).
[27] O. Gühne and G. Tóth, Phys. Rep. **474**, 1 (2009).
[28] M. El Khatib, O. Brea, E. Fertitta, G. L. Bendazzoli, S. Evangelisti, T. Leininger, and B. Paulus, Theor. Chem. Acc. **134**, 1 (2015).
[29] J. Hubbard, Proc. R. Soc. A **276**, 238 (1963).
[30] H. Schulz, Phys. Rev. Lett. **64**, 2831 (1990).
[31] V. I. Anisimov, J. Zaanen, and O. K. Andersen, Phys. Rev. B **44**, 943 (1991).
[32] R. Bulla, Phys. Rev. Lett. **83**, 136 (1999).
[33] S. Pankov and V. Dobrosavljević, Phys. Rev. B **77**, 085104 (2008).
[34] L. Stella, C. Attaccalite, S. Sorella, and A. Rubio, Phys. Rev. B **84**, 245117 (2011).
[35] F. Mancini, E. Plekhanov, and G. Sica, Eur. Phys. J. B **86**, 1 (2013).
[36] Y.-Y. Li, J. Cao, W.-L. Yang, K. Shi, and Y. Wang, Nucl. Phys. B **879**, 98 (2014).
[37] M. Imada, A. Fujimori, and Y. Tokura, Rev. Mod. Phys. **70**, 1039 (1998).
[38] N. F. Mott, J. Solid State Chem. **88**, 5 (1990).
[39] J. Hachmann, W. Cardoen, and G. K.-L. Chan, J. Chem. Phys. **125**, 144101 (2006).
[40] T. Tsuchimochi and G. E. Scuseria, J. Chem. Phys. **131**, 121102 (2009).
[41] A. V. Sinitskiy, L. Greenman, and D. A. Mazziotti, J. Chem. Phys. **133**, 014104 (2010).
[42] A. E. DePrince III, M. Pelton, J. R. Guest, and S. K. Gray, Phys. Rev. Lett. **107**, 196806 (2011).
[43] D. A. Mazziotti, Phys. Rev. Lett. **106**, 083001 (2011).
[44] R. Kubo, J. Phys. Soc. Jpn. **17**, 1100 (1962).
[45] T. A. Severini, *Elements of Distribution Theory* (Cambridge University Press, 2005), Vol. 17.
[46] S. Rao Jammalamadaka, T. Subba Rao, and G. Terdik, Sankhy Indian J. Stat. **68**, 326 (2006).
[47] C. Angeli, G. L. Bendazzoli, and S. Evangelisti, J. Chem. Phys. **138**, 054314 (2013).
[48] See supplementary material at http://dx.doi.org/10.1063/1.4913734 for energies, position spreads, polynomial fitting, and the analytical treatment of the hydrogen dimer.
[49] S. J. Van Enk, Phys. Rev. A - At. Mol. Opt. Phys. **72**, 1 (2005).

[50]NEPTUNUS is a FORTRAN code for the calculation of FCI energies and properties written by Bendazzoli, G. L. and Evangelisti, S. with contributions from Gagliardi, L., Giner, E., Monari, A., and Verdicchio, M.

[51]G. L. Bendazzoli and S. Evangelisti, J. Chem. Phys. **98**, 3141 (1993).

[52]G. L. Bendazzoli and S. Evangelisti, Int. J. Quantum Chem. **48**, 287 (1993).

[53]L. Gagliardi, G. L. Bendazzoli, and S. Evangelisti, J. Comput. Chem. **18**, 1329 (1997).

[54]Dalton A Molecular Electronic Structure Program. See: http://www.kjemi.uio.no/software/dalton/dalton.html, 2005.

[55]C. Angeli, G. L. Bendazzoli, S. Borini, R. Cimiraglia, A. Emerson, S. Evangelisti, D. Maynau, A. Monari, E. Rossi, J. Sanchez-Marin, P. G. Szalay, and A. Tajti, Int. J. Quantum Chem. **107**, 2082 (2007).

[56]S. Borini, A. Monari, E. Rossi, A. Tajti, C. Angeli, G. L. Bendazzoli, R. Cimiraglia, A. Emerson, S. Evangelisti, D. Maynau, J. Sanchez-Marin, and P. G. Szalay, J. Chem. Inf. Model. **47**, 1271 (2007).

[57]S. Rampino, A. Monari, E. Rossi, S. Evangelisti, and A. Laganà, Chem. Phys. **398**, 192 (2012).

[58]E. Rossi, S. Evangelisti, A. Laganà, A. Monari, S. Rampino, M. Verdicchio, K. K. Baldridge, G. L. Bendazzoli, S. Borini, R. Cimiraglia, C. Angeli, P. Kallay, H. P. Lüthi, K. Ruud, J. Sanchez-Marin, A. Scemama, P. G. Szalay, and A. Tajti, J. Comput. Chem. **35**, 611 (2014).

[59]E. Lieb and F. Wu, Phys. Rev. Lett. **20**, 1445 (1968).

[60]T. H. Dunning, J. Chem. Phys. **90**, 1007 (1989).

[61]D. Tunega and J. Noga, Theor. Chim. Acta **100**, 78 (1998).

[62]C. C. J. Roothaan, J. Chem. Phys. **19**, 1445 (1951).